



BIONATURE 2016

The Seventh International Conference on Bioenvironment, Biodiversity and
Renewable Energies

ISBN: 978-1-61208-489-3

ENVIROSENS 2016

The International Symposium on Remote Sensing for Climate and Earth Monitoring

June 26 - 30, 2016

Lisbon, Portugal

BIONATURE 2016 Editors

Birgit Gersbeck-Schierholz, Leibniz Universität Hannover, Germany

Michael Byalsky, The Hebrew University of Jerusalem, Israel

BIONATURE 2016

Foreword

The Seventh International Conference on Bioenvironment, Biodiversity and Renewable Energies (BIONATURE 2016), held between June 26 - 30, 2016 - Lisbon, Portugal, covered these two main areas: environment and renewable and sustainable energies.

Environmental change awareness is a key state of spirit and legislation for preventing, protecting, and ultimately saving the planet biodiversity. Technical and practical methods for applying bio-agriculture for the public's health and safety are primary targets. The goal is the use of ecological economic stimuli in tandem with social and governmental actions preventing deforestation, pollution, and global warming. To cope with the climate and landscape changes advanced technical inventory of tools and statistics on lessons learned are needed to derive appropriate measure and plan accordingly.

Replacing the classical energy with alternative renewable energy (green energy), such as bioenergy, eolian energy, or solar energy is an ecological and economic trend that suggests important socio-economic advantages: using native renewable resources, increasing of self-sufficiency rate of energy and promoting use of clean energy, and that way, polluting emissions to the air will be reduced. Bioenergy is renewable energy derived from biological sources, to be used for heat, electricity, or vehicle fuel. Biofuel derived from plant materials is among the most rapidly growing renewable energy technologies. In several countries corn-based ethanol is currently the largest source of biofuel as a gasoline substitute or additive. Recent energy legislation mandates further growth of both corn-based and advanced biofuels from other sources. Growing biofuel demand has implications for U.S. and world agriculture. Eolian energy is currently used throughout the world on a large scale. In the past decade, its evolution shows its acceptance as a source of generation, with expressive growth trends in the energy matrices in the countries where this source is used Eolian energy is renewable and has very low environmental impact. To generate it, there are no gas emissions, no effluent refuse, and no other natural resources, such as water, are consumed. Photovoltaic technology makes use of the energy in the sun, and it has little impact on the environment. Photovoltaics can be used in a wide range of products, from small consumer items to large commercial solar electric systems. The event brought together the challenging technical and regulation aspects for supporting and producing renewable energy with less or no impact on the ecosystems. There are several technical integration barriers and steps for social adoption and governmental legislation to favor and encourage this kind of energy.

The BIONATURE 2016 conference also featured the following symposium:

- ENVIROSENS 2016 - The International Symposium on Remote Sensing for Climate and Earth Monitoring

We take here the opportunity to warmly thank all the members of the BIONATURE 2016 Technical Program Committee, as well as the numerous reviewers. The creation of such a high quality conference program would not have been possible without their involvement. We also kindly thank all the authors who dedicated much of their time and efforts to contribute to BIONATURE 2016. We truly believe that, thanks to all these efforts, the final conference program consisted of top quality contributions.

Also, this event could not have been a reality without the support of many individuals, organizations, and sponsors. We are grateful to the members of the BIONATURE 2016 organizing

committee for their help in handling the logistics and for their work to make this professional meeting a success.

We hope that BIONATURE 2016 was a successful international forum for the exchange of ideas and results between academia and industry and for the promotion of progress in the fields of bioenvironment and renewable energies.

We also hope that Lisbon provided a pleasant environment during the conference and everyone saved some time for exploring this beautiful city.

BIONATURE 2016 Chairs:

Suhkneung Pyo, Sungkyunkwan University - Suwon City, South Korea

Vladimir Strezov, Macquarie University - Sydney Australia

Victor Zaichenko, Biocenter, Russia

BIONATURE 2016

Committee

BIONATURE Advisory Committee

Suhkneung Pyo, Sungkyunkwan University - Suwon City, South Korea
Vladimir Strezov, Macquarie University - Sydney Australia
Victor Zaichenko, Biocenter, Russia

BIONATURE 2016 Technical Program Committee

Silvia Assini, University of Pavia, Italy
Yoseph Bar-Cohen, NDEAA - Jet Propulsion Lab (JPL) - NASA, USA
Michael Byalsky, The Hebrew University of Jerusalem, Israel
Rupp Carriveau, University of Windsor, Canada
Longjian Chen, China Agricultural University, China
Gianfranco Chicco, Politecnico di Torino, Italy
Pedro Corrêa, University of São Paulo, Brazil
Hany A. El-Shemy, Cairo University - Giza, Egypt
Jerekias Gandure, University of Botswana, Botswana
Josean Garrués Irurzun, University of Granada, Spain
Giuseppe Genon, Politecnico di Torino, Italy
Bassim H. Hameed, University of Science Malaysia - Penang, Malaysia
Kathleen Hefferon, Cornell University, USA
Ana Jesús López, University of Oviedo, Spain
Man Kee Lam, Universiti Teknologi PETRONAS - Perak, Malaysia
Arie Lavie, CTI - Creative Technologies Israel, Israel
Valentinas Klevas, Kaunas University of Technology / Lithuanian Energy Institute, Lithuania
José Augusto Medrano Hernandez, Centro de Estudio de Tecnologías Energéticas Renovables (CETER) - CUJAE, Cuba
Abdeen Mustafa Omer, Energy Research Institute (ERI) - Khartoum, Sudan
Son V. Nghiem, Jet Propulsion Laboratory, California Institute of Technology - Pasadena, USA
Patrícia Pereira da Silva, University of Coimbra & INESC-Coimbra, Portugal
Suhkneung Pyo, Sungkyunkwan University - South Korea
Bale V. Reddy, University of Ontario Institute of Technology - Oshawa, Canada
Francisca Segura Manzano, University of Huelva, Spain
Atul Sharma, Rajiv Gandhi Institute of Petroleum Technology - Rae Bareilly, India
Vladimir Strezov, Macquarie University - Sydney Australia
Lee Keat Teong, Universiti Sains Malaysia - Penang, Malaysia
Shuki Wolfus, Bar-Ilan University, Israel
Talal Yusaf, University of Southern Queensland - Toowoomba, Australia
Victor Zaichenko, Biocenter, Russia

ENVIROSENS 2016 Program Committee Members

Thierry Badard, Centre for Research in Geomatics - Laval University, Quebec, Canada
Elena Camossi, NATO STO Centre for Maritime Research and Experimentation, Italy
Beata Csatho, University at Buffalo, USA
Gabriel de Oliveira, Brazilian National Institute for Space Research (INPE), Brazil
Lúcio André de Castro Jorge, Embrapa Instrumentação, Brazil
Gerrit de Leeuw, Finnish Meteorological Institute / University of Helsinki, Finland
Fabio Del Frate, University of Rome Tor Vergata, Italy
Oleg Dubovik, Universite Lille-1, France
Guido D'Urso, Universita' degli Studi di Napoli Federico II, Italy
Garik Gutman, NASA Land-Cover / Land-Use Change Program, USA
Shahid Habib, NASA - Goddard Space Flight Center, USA
Irena Hajsek, ETH Zurich, Switzerland / German Aerospace Center, Germany
Sergio Ilarri, University of Zaragoza, Spain
Shuanggen Jin, Shanghai Astronomical Observatory / Chinese Academy of Sciences, China
Martin Kappas, Institute of Geography - Georg-August University Goettingen, Germany
Alexander Kokhanovsky, EUMETSAT, Germany
Kati Laakso, Specim Ltd., Finland
Jonathan Li, University of Waterloo, Canada
Andrea Masini, Flyby S.r.l., Italy
Alberto Moreira, German Aerospace Center (DLR) / Karlsruhe Institute of Technology (KIT), Germany
Alberto Ortolani, CNR-IBIMET (Italian National Research Council - Institute of BioMeteorology) / LaMMA Consortium (Laboratory of Environmental Monitoring and Modelling for the sustainable development), Italy
Alenka Poplin, Iowa State University, USA
Kamel M. Sheikho, King Abdulaziz City for Science and Technology (KACST), Saudi Arabia
Haruhisa Shimoda, Tokai University Research & Information Center, Japan
Todd Shipman, Alberta Energy Regulator (AER) / Alberta Geological Survey, Canada
Cyril Voyant, Université de Corse, France
Francesco Vuolo, University of Natural Resources and Life Sciences, Vienna (BOKU), Austria

Copyright Information

For your reference, this is the text governing the copyright release for material published by IARIA.

The copyright release is a transfer of publication rights, which allows IARIA and its partners to drive the dissemination of the published material. This allows IARIA to give articles increased visibility via distribution, inclusion in libraries, and arrangements for submission to indexes.

I, the undersigned, declare that the article is original, and that I represent the authors of this article in the copyright release matters. If this work has been done as work-for-hire, I have obtained all necessary clearances to execute a copyright release. I hereby irrevocably transfer exclusive copyright for this material to IARIA. I give IARIA permission to reproduce the work in any media format such as, but not limited to, print, digital, or electronic. I give IARIA permission to distribute the materials without restriction to any institutions or individuals. I give IARIA permission to submit the work for inclusion in article repositories as IARIA sees fit.

I, the undersigned, declare that to the best of my knowledge, the article does not contain libelous or otherwise unlawful contents or invading the right of privacy or infringing on a proprietary right.

Following the copyright release, any circulated version of the article must bear the copyright notice and any header and footer information that IARIA applies to the published article.

IARIA grants royalty-free permission to the authors to disseminate the work, under the above provisions, for any academic, commercial, or industrial use. IARIA grants royalty-free permission to any individuals or institutions to make the article available electronically, online, or in print.

IARIA acknowledges that rights to any algorithm, process, procedure, apparatus, or articles of manufacture remain with the authors and their employers.

I, the undersigned, understand that IARIA will not be liable, in contract, tort (including, without limitation, negligence), pre-contract or other representations (other than fraudulent misrepresentations) or otherwise in connection with the publication of my work.

Exception to the above is made for work-for-hire performed while employed by the government. In that case, copyright to the material remains with the said government. The rightful owners (authors and government entity) grant unlimited and unrestricted permission to IARIA, IARIA's contractors, and IARIA's partners to further distribute the work.

Table of Contents

On the Wind Turbines Assessment by Real Options Technique in Israel <i>Doron Greenberg, Michael Byalsky, and Asher Yahalom</i>	1
A New Improvement of the Naturalistic Indicator of Forest Quality. An Italian Case Study <i>Silvia Assini and Maria Grazia Albanesi</i>	7
The Assessment of Environmental Changes of Selected Water Bodies in the Area of Cracow over the Past Two Decades <i>Aleksandra Wagner, Peter Eggenbauer, Aleksandra Obrist, and Boris Tokmacija</i>	11
Analysing the fAPAR Dynamic Over Europe Using MODIS Data <i>Carmelo Cammalleri, Fabio Micale, and Jurgen Vogt</i>	17
Aerial Image Mosaics Construction Using Heterogeneous Computing for Agricultural Applications <i>Leandro Rosendo Candido, Maximilian Luppe, and Lucio Andre de Castro Jorge</i>	22

On the Wind Turbines Assessment by Real Options Technique in Israel

Doron Greenberg

Department of Economics & Business Administration
Ariel University
Ariel, Israel
e-mail: dorongre@ariel.ac.il

Michael Byalsky

Department of Economics
The Hebrew University of Jerusalem
Jerusalem, Israel
e-mail: michael.byalsky@mail.huji.ac.il

Asher Yahalom

Department of Electrical & Electronics Engineering
Ariel University
Ariel, Israel
e-mail: asya@ariel.ac.il

Abstract— The limitation factor for using of the local energy resources in Israel is the persistent one that causes different economics participants to develop the ‘green’ technologies. The wind turbines installation constitutes undoubtedly an important trend of their efforts in this area. Many methods are elaborated for assessment of the investment projects in the industry and energetics. One of them, extensively applied to the investments evaluation, presents the standard discounted cash flow method, using the net present value criterion. Yet, this method is unsuitable for the fast altering investment environment, and for the consequent need of the managerial decisions flexibility. The technique of real options analysis is broadly used nowadays in many investment projects of renewable energy for their efficiency estimating. The current research develops the real options analysis facilities for evaluation of the wind turbines efficiency and profitability, as a part of the wind energy economic potential in Israel.

Keywords— wind energy; energy market; renewable energy; investment decisions; real option analysis

I. INTRODUCTION

Nowadays, considering the Israeli energy market, even when such plentiful sources of traditional nonrenewable energy as the prominent gas fields discovered in the Mediterranean Sea off the coast of Israel: the Tamar [1] and the Leviathan [2] gas fields with the estimated stocks of 356 and 450 billion cubic meters respectively, - the perspective of their exhaustion still forces the state, as other numerous countries, to devote various efforts to the ‘green’ energy research and development. These efforts are undertaken primarily in the area of solar energy, but also last period in wind energy installations. Yet the wind power amount produced in Israel is diminutive comparing to the continuously growing world global market, however, the last steps undertaken by the state are designed to improve the situation.

Israel currently operates one wind farm in Asanyia Hill in the Golan Heights, with an installed capacity of 6 MW (10 turbines at a height 50 meters including blades, each

with a capacity of 600 kW), consumption of about 5 thousand families. The duty cycle of the wind farm operating reaches 97%, and electricity selling consists 1 million US \$ a year. Indeed, wind energy potential of Israel is restricted due to moderate- or poor-wind velocities’ areas, and is limited to the areas with sufficiently high average wind speed, some of which are being opposed by green groups on landscape conservation grounds. Anyhow, in accordance with the Israel Ministry of Environmental Protection (IMEP) directions, the state continues efforts for the development of two more farms with a 50 MW capacity [3].

As it is emphasized in a document of the Israeli Knesset (Parliament), an improved estimate, based on the wind turbines’ technological development, gives a value higher than 500 MW for the Israeli potential wind energy capacity [4].

The main goal of this paper is the study of the influence of energy price fluctuations on the assessment of the feasibility wind turbine installation using the real option analysis tool.

The economic output of wind turbine field is a function of its electric power output and market energy prices, when the electric power output is a function of the equipment used and wind velocity statistics.

The equipment can be chosen to have an optimal *cut-in speed* (the wind speed level at which the turbine begins to generate electricity), and the *cut-out speed* (the speed level at which the turbine hits its alternator limit and intermits to produce increased power output following increases in a wind speed) [5]. For a more detailed discussion, we refer the reader to results of our previous investigations of the wind energy use, devoted to the technical appropriateness and environmental relevance questions [6]-[9].

While the annual power output of the field can be known to a high certainty degree, the prices of energy may vary indeterminately, and thus should be considered as a prominent investment risk. To evaluate the influence of risk

correctly we suggest the real option analysis which is the subject of this paper.

In this context, our purpose is to contribute to the way where, following Grossman’s conception of risk allocation, "decentralized economy allocates risk and investment resources when information is dispersed" [10, p. 773].

Thus, in Section II, we describe the results of our preliminary statistic survey and the estimation results based on the investigated area’s data. In Section III, we outline and apply the methods of the wind energy exploitation’s estimation using the real options technique. Section IV is devoted to the analysis of energy prices’ volatility in general and in Israel particularly. In Section V, we complete the use of the real options analysis for the wind turbines assessment in a case of high variability applying to the given data, and in Conclusion, we summarize the main obtained results.

II. STATISTIC ESTIMATION RESULTS

In the general framework of our research, we concentrated on the wind velocity distribution at the Golan Heights region, using the data of the Meteorological Service of the Israel Ministry of Transport and Road Safety [11], collected by the Merom Golan meteorological station, one of the 84 Israeli stations which is situated at the given area [12], for the 2014 year. The data include 52,066 observations during this period of time, the sample values of the wind speed, one observation for every 10 minutes, 144

values per day (except some non-significant missing values) [13].

We used the Weibull distribution function as the common accepted most appropriate function describing the wind speed statistical frequencies at a given location in most of the world. This information is essential for the planning of the wind turbine optimal configuration [6].

Generally, the Weibull probability distribution function (PDF) is defined, concerning a random variable of the wind speed X , by two parameters. They are a *shape parameter* k (dimensionless) and a *scale parameter* λ (m/s for the wind speed), which together determine the PDF form, as follows:

$$f(x; \lambda, k) = \begin{cases} \frac{k}{\lambda} \left(\frac{x}{\lambda}\right)^{k-1} e^{-\left(\frac{x}{\lambda}\right)^k}, & x \geq 0 \\ 0, & x = 0 \end{cases} \quad (1)$$

The PDF parameter values in (1) are significant for choosing the optimal location for the wind turbine, as well as for selecting most efficient turbine, which imply the wind farm efficiency [14].

For fitting the observed data of the given location to the PDF [15], we used the method of the maximum likelihood estimators [16]. The corresponding Weibull PDF for the wind speeds distribution at the Merom Golan site, together with their distribution histogram, is shown below in Figure 1.

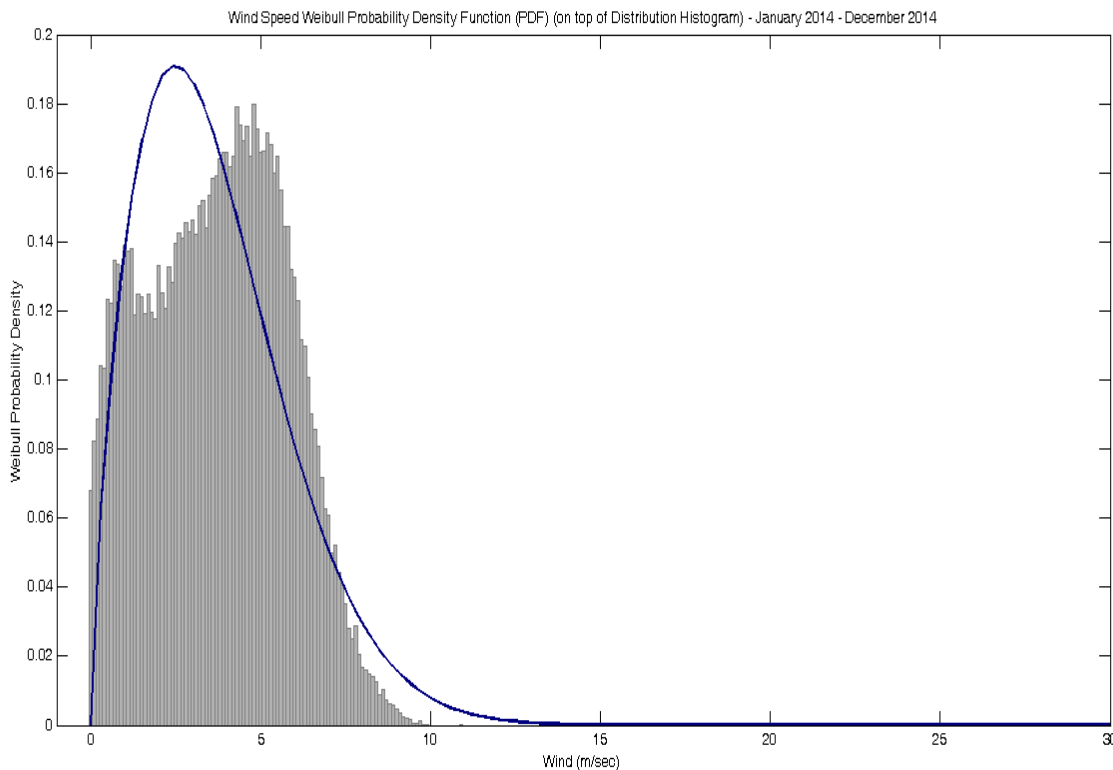


Figure 1. The Weibull PDF diagram for the Merom Golan wind speeds distribution (on top of distribution histogram).

The figure demonstrates visually that low and moderate winds are widespread, with a tight condensation at the primary segment, which means that storms are just rare. It should be noticed that the distribution approximation by a Weibull PDF in this case is not perfect, though we could however obtain approximately based on it, the wind principal statistical parameters.

Estimated annual parameters of the wind Weibull distribution were found to be: $k=1.7228$ and $\lambda=4.1206$ m/s. In addition we calculated (excess) kurtosis (a measure of the PDF sharpness) to be 2.1757, and skewness (a measure of the PDF asymmetry) as 0.0574, were calculated to demonstrate the specific type of the Weibull PDF.

The main meaningful statistical parameter for planning of the wind turbine installation, the speed mean, was obtained of 3.73 m/s, with Standard deviation of 2.03, during the given period, with a positive right-skewed tail. This finding, in accordance to the Israeli Cooperative for Renewable Energy conclusions [17], indicates the possibility of wind energy exploitation in the investigated region.

III. USING OF THE REAL OPTIONS ANALYSIS FOR THE WIND ENERGY EXPLOITATION'S ESTIMATION

While the standard discounted cash flow (DCF) method using the net present value (NPV) criterion is extensively adopted to evaluate investments, the standard DCF method is inappropriate for a rapidly changing investment climate (Dixit and Pindyck [18]; Herath and Park [19]; Lee and Shih [20]) and for the managerial flexibility in investment decisions (Hayes and Abernathy [21]; Hayes and Garvin [22]; Trigeorgis and Mason [23]; Trigeorgis [24]).

In recent years, the real options analysis technique is widely applied in many studies for valuation of renewable energy investment projects, for example Lee and Shih [20], Kumbaroğlu, Madlener and Demirel [25], Boomsma, Meade and Fleten [26], Menegaki [27]. Hence, we apply in this study the real options analysis approach for the valuation of wind energy turbines. In particular, we capture the value of the follow-on investment opportunities which add value to the investment.

We found in our study on the basic Black-Scholes model of a financial market [28], because we focus on the missing value of the option to abandon in an environment where it is impossible to estimate the standard deviation by the numerical tools.

We analyze in the current study the feasibility of installing an additional turbine field in the Asanyia Hill in the Golan Heights, in order to extract value from wind. We have partly based our investigation on the achieved results of the wind turbines construction and exploitation in Israel [29], while some of the numbers presented here are rough estimates. The decision to build the field which encompasses many turbines can be divided into two stages: in the 1st stage, we build one unit. After building and operating which may take few years, the 2nd decision on

building the turbine field is taken based on electricity price at this stage.

We model the uncertainty over future electricity prices as a price of an underlying asset of a real option using Black-Scholes formula (2) as in [28]:

$$C = S_0 N(d_1) - K e^{-rT} N(d_2), \tag{2}$$

where

$$d_1 = \frac{\ln(S_0 / K) + (r + \sigma^2 / 2)T}{\sigma \sqrt{T}}, \tag{3}$$

$$d_2 = \frac{\ln(S_0 / K) + (r - \sigma^2 / 2)T}{\sigma \sqrt{T}} = d_1 - \sigma \sqrt{T}.$$

The notations in (2), (3) above are as follows:

C is the call option value, S_0 is the price of the underlying asset, K is the exercise price, r is the annual risk free return, T is the duration of the period (the number of years) till exercising the option, and σ is the annualized standard deviation (StD) of the return of the underlying asset. N stands for the normal distribution cumulative density function (CDF).

All the used figures were elaborated in accordance with a proposed scenario as in a Table I below, where the real figures can be introduced according to the data of each project (all costs are given in millions \$US).

We apply here the technique of real option valuation as illustrated in Brealey et al. [30, p. 584], where we have replaced:

TABLE I. INPUT DATA FOR THE BLACK-SCHOLES OPTION VALUE CALCULATION

Data for the Black-Scholes Option Value	
Cost of the 1 st stage's one turbine building	50
Annual turbine's profit in the 2 nd stage	0.2
Present value of 50 turbines' profit over 20 years = Stock Price now (S_0)	114.7
Cost of the 2 nd stage's for each turbine construction	1.2
Number of turbines in the 2 nd stage (entire field)	50
Cost of the 2 nd stage's 50 turbines building = Exercise Price of Option (K)	60
Number of Periods to Exercise in years (T)	2
Compounded Risk-Free Interest Rate (r)	0.02
Standard Deviation of prices of energy or electricity (annualized σ)	0.031

- the stock price with the current value of the field, $S_0=114.7$ million \$US, which is the present value of 20 years future operation with annual profit of 0.2 million \$US per turbine for a field of 50 turbines, discounted with 6% annual cost of capital;

- the number of periods to exercise in years (T) with the number of years between confirmation of 1st stage (one unit) to the decision on the 2nd stage (the field).

We have therefore calculated firstly the call value, based on the annual StD estimation of 0.031, as 57.05 million \$US. This StD estimation of 0.031 is based on the data of the Electric Power Monthly report of the U.S. Energy Information Administration (EIA), Table 5.3 “Average Retail Price of Electricity to Ultimate Customers” [31].

Our assumption of the 1st unit’s building cost is equaled, as above mentioned, to 50 million \$US, where such high expenses of the first turbine’s launching include, among others, research and development to adapt the turbine to the specific area under consideration and the cost of connecting it to the power grid, subtracted by the profit from operation.

Hence, the results indicate that the investment in the 1st turbine stage is warranted, and that there is the option to follow on, which adds significant value to the investment. It follows that the net profit of the 1st stage is $57.05-50 = 7.05$ million \$US for the standard deviation value of 0.031, accordingly to the following data of a Table II (in a column for the StD = 0.031 case), which includes the intermediate values and the option to follow-on.

For comparison with a scenario lacking an option to abandon, the project value is estimated as the present discounted value of a difference between (i.e., the earnings from) the future cash flow raised from the 2nd stage realization subtracted by the 2nd stage building cost, which subtracted additionally by the 1st stage building cost.

Applying to our numerical example, this yields just the negative benefit, meaning merely loss, of the $(114.7-60)/1.06^2 - 50 = -1.3$ million \$US.

However, using StD of 0.031 yields a profit of 7.05 million \$US, as was calculated above. This is so because one can make a choice to abandon the project in its midst. This is the economic meaning of the real option.

TABLE II. INTERMEDIATE AND OUTPUT DATA FOR THE BLACK-SCHOLES OPTION VALUE

Intermediate and Output Data		
StD	0.031	0.40
$\sigma\sqrt{T}$	0.0438	0.5657
$d1$	15.7146	1.4990
$d2$	15.6707	0.9333
Delta $N(d1)$ Normal CDF	0.5123	0.9331
Value of the Call Option to Follow-On	57.05	59.48

IV. ESTIMATING THE VOLATILITY OF ENERGY PRICES

It is difficult to determine the direction and intensity of energy prices in the future. For example, the U.S. Energy Information Administration in its "Independent Statistics & Analysis" publication "The Availability and Price of Petroleum and Petroleum Products Produced in Countries other than Iran" states:

"The uncertainty on both the supply and demand side of the market could result in large future price movements [underlined by the authors]. The possible lifting of sanctions on Iran could move additional supply on to the world market and reduce prices, while an unexpected supply disruption at a time of low surplus production capacity may push prices higher" [32]. Such irregular fluctuations in supply and demand can be observed in the graph from this report in Figure 2, where the spread between production and consumption is widening since July 2014.

In addition to the world energy price uncertainty, there are at least four other sources for price uncertainty in Israel: (a) the possibility of military conflict; (b) the discovery of gas in Israel's shore; (c) the adoption of gas by the industry; For example, Foenicia – a glass manufacturer that was recently close to bankruptcy due to lack of gas turned to be a profitable [33]; and (d) the discovery of oil in the Golan Heights [34].

While it is still difficult with all these sources of uncertainty to determine the direction and intensity of the change of energy price, we must consider thus the possibility of high volatility in price. To this end, we will consider hereafter the possibility of high volatility taken to be StD=40% per annum.

V. USING OF THE REAL OPTIONS ANALYSIS FOR THE WIND ENERGY EXPLOITATION’S ESTIMATION WITH HIGH VOLATILITY

Calculating the call value, based on the annual StD estimation of 0.4, yields 59.48 million \$US (compared to 57.05 million \$US based on StD of 0.031).

It follows that the net profit of the 1st stage increased to $59.48-50 = 9.48$ million \$US (see Table II, a column for the StD = 0.40 case).

It would be worth to notice here that the main statistical parameters of the wind speed at the Merom Golan area, the mean and StD, are observed with a tendency to stability, without any significant divergence over the period of last years 2009-2014, as it follows from the calculated at the Table III data.

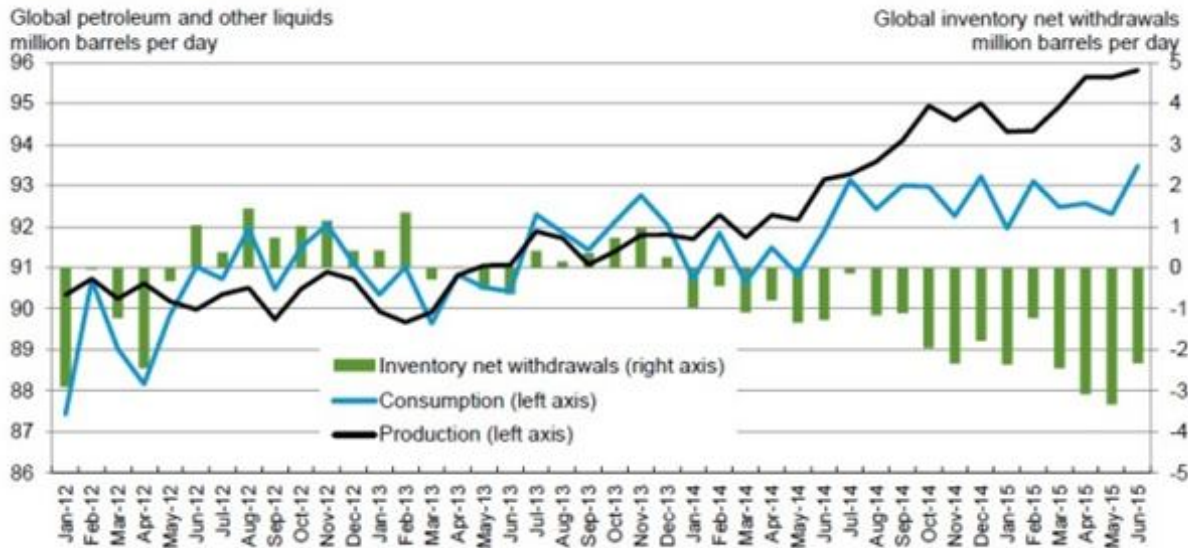


Figure 2. Global Petroleum and other Liquids Production, Consumption and Inventory Net Withdrawals, January 2012-June 2015 [32].

The expectation value of an annual average is the same as the expectation value for one sample but the standard deviation of the annual average is equal to the standard deviation of one sample divided by the square root of the annual number of samples. Thus, the standard deviation of the annual average of wind speed is between 0.6%-1.1% and can be further reduced by more sampling. A six year average based on 24327 samples will be 3.72 m/s with only 0.4% standard deviation.

The standard deviation of average power for all turbines investigated is much lower than the mentioned above standard deviations. Hence, a long term project can ignore the risk connected with the standard deviation of wind speed.

This circumstance determines the fact of non-relevancy of the speed variance, during prolonged period of time, for the wind turbine economic value; this should be compared to the significance of the energy prices for the turbine economic value.

TABLE III. WIND SPEED MEAN AND STD AT MEROM GOLAN FOR THE LAST PERIOD

Year	2009	2010	2011	2012	2013	2014
Speed mean (m/s)	3.89	3.69	3.63	3.70	3.80	3.62
StD (m/s)	2.10	2.12	2.00	2.03	2.05	1.99
Number of Samples	2919	2920	2920	9774	2896	2898
StD/\sqrt{n} (m/s)	0.039	0.039	0.037	0.021	0.038	0.037

VI. CONCLUSION

Traditional calculation for an uncertain cash flow applies just the expected values of the cash flow from the project without the possibility to abandon. Given our empirical assumptions, this yields a loss of 1.3 million \$US instead of any profit, meaning the project becomes not worthwhile.

Contrariwise, applying the proposed real option analysis, which reveals the value of the option to abandon the 2nd stage running as well, we turn the project just to become profitable and worthwhile. The value of the real option increases depending volatility to be either 57.05 million \$US or 59.50 million \$US depending on future volatility, and the profit is either 7.05 million \$US or 9.48 million \$US, respectively.

REFERENCES

- [1] "Tamar gas field," Wikipedia. Retrieved: May, 2016, from http://en.wikipedia.org/wiki/Tamar_gas_field.
- [2] "Leviathan gas field," Wikipedia. Retrieved: May, 2016, from http://en.wikipedia.org/wiki/Leviathan_gas_field.
- [3] "Renewable energy," Israel Ministry of Environmental Protection. [Electronic version]. Retrieved: April, 2016, from <http://www.sviva.gov.il>.
- [4] O. Lotan, "Wind energy power generation," Background paper, 21.09.05 (in Hebrew). Jerusalem: Knesset, Research and Information Center, 2005.
- [5] P. Gray and L. Johnson (1985). Wind Energy System. Upper Saddle River, NJ: Prentice Hall, 1985.
- [6] M. Byalsky and A. Yahalom, "Modeling of the Wind Energy Use Efficiency", The 4th Annual International Conference on Qualitative and Quantitative Economics Research (QQE 2014), GSTF, Phuket, Thailand, 28-29th Apr., 2014, pp. 91-93.
- [7] Y. Ditkovich, A. Kuperman, A. Yahalom, and M. Byalsky, "A Generalized Approach to Estimating Capacity Factor of Fixed Speed Wind Turbines", IEEE Transactions on Sustainable Energy (2012), Vol. 3 (3), pp. 607-608, doi:10.1109/TSTE.2012.2187126.
- [8] Y. Ditkovich, A. Kuperman, A. Yahalom, and M. Byalsky, "Site-Dependent Wind Turbine Performance Index",

- International Journal of Renewable Energy Research (2013), Vol. 3 (3), pp. 592-594.
- [9] Y. Ditkovich, A. Kuperman, A. Yahalom, and M. Byalsky, "Alternative Approach to Wind Turbine Performance Index Assessment", *Journal of Energy Engineering* (2014), Vol. 140 (4), 06014001, pp. 1-4.
- [10] S.J. Grossman, "Dynamic Asset Allocation and the Informational Efficiency of Markets", *The Journal of Finance* (1995), Vol. 50 (3), pp. 773-787.
- [11] "The Israel Meteorological Service Site". Retrieved: May, 2016, from http://www.ims.gov.il/ims/all_tahazit/.
- [12] "The Israel Meteorological Stations' Characteristics". Retrieved: May, 2016, from <https://data.gov.il/sites/data.gov.il/files/metadata10minutesIMS7.XLSX>.
- [13] "The Government Information Data Bases' Site". Retrieved: May, 2016, from <https://data.gov.il/ims/7>.
- [14] "Weibull statistics," *Reliability Engineering*. Retrieved: April, 2016, from <http://www.weibull.nl/weibullstatistics.htm>.
- [15] P. Bhattacharya and R. Bhattacharjee, "A study on Weibull distribution for estimating the parameters", *Journal of Applied Quantitative Methods* (2010), Vol. 5 (2), pp. 234-241.
- [16] "Weibull Parameter Estimates", *MathWorks Documentation Center*. [Electronic version]. Retrieved: May, 2016, from www.mathworks.com/help/toolbox/stats/wblfit.html.
- [17] H. Levy, "Installation of small wind turbines for the electricity generation," *Israeli Cooperative for Renewable Energy* (in Hebrew). [Electronic version]. Retrieved: May, 2016, from http://ecoop.org.il/index.php?option=com_content&view=article&id=88&Itemid=135.
- [18] A.K. Dixit and R.S. Pindyck, "The options approach to capital investment", *Harv. Bus. (1995)*, Rev. 73 (3), pp. 105-115.
- [19] H.S.B. Herath and C.S. Park, "Economic Analysis of R&D projects: an options approach", *Eng. Econ.* (1999), Vol. 44 (1), pp. 1-35.
- [20] Shun-Chung Lee and Li-Hsing Shih, "Renewable energy policy evaluation using real option model — The case of Taiwan," *Energy Economics* (2010), Vol. 32, (S1), pp. 67-78.
- [21] R.H. Hayes and W.J. Abernathy, "Managing our way to economic decline", *Harv. Bus. (1980)*, Rev. 58 (4), pp. 67-77.
- [22] R.H. Hayes and D. Garvin, "Managing as it tomorrow mattered", *Harv. Bus. (1982)*, Rev. 60 (3), pp. 70-79.
- [23] L. Trigeorgis and S.P. Mason, "Valuing managerial flexibility and strategy in resource", *Midl. Corp. Financ. J.*, (1987), Vol. 5 (1), pp. 14-21.
- [24] L. Trigeorgis, "Real Option: Managerial Flexibility and Strategy, Resource Allocation", 2nd ed., Parager Publisher, Westport, 1997.
- [25] G. Kumbaroğlu, R. Madlener, and M. Demirel, "A real options evaluation model for the diffusion prospects of new renewable power generation technologies", *Energy Economics* (2008), Vol. 30 (4), pp. 1882-1908.
- [26] T.K. Boomsma, N. Meade, and S.-E. Fleten, "Renewable energy investments under different support schemes: A real options approach", *European Journal of Operational Research* (2012), Vol. 220 (1), pp. 225-237.
- [27] A. Menegaki, "Valuation for renewable energy: a comparative review", *Renewable and Sustainable Energy Reviews* (2008), Vol. 12 (9), pp. 2422-2437.
- [28] F. Black and M. Scholes, "The pricing of options and corporate liabilities," *The Journal of Political Economy* (1973), Vol. 81 (3), pp. 637-654.
- [29] "Wind Energy Golan" [Electronic version]. Retrieved: May, 2016, from <http://www.wind-golan.com/>.
- [30] R. A. Brealey, S. C. Myers, and F. Allen. "Principles of corporate finance," 10th ed., New York: McGraw-Hill/Irwin, 2011.
- [31] "Electric Power Monthly Report of the U.S. Energy Information Administration (EIA)", *Electricity*. Retrieved: May, 2016, from http://www.eia.gov/electricity/?m&t=epmt_5_03.
- [32] "The Availability and Price of Petroleum and Petroleum Products Produced in Countries Other Than Iran". No. 23 in a series of reports required by section 1245(d)(4)(A) of the National Defense Authorization Act for Fiscal Year 2012. Retrieved: May, 2016, from <http://www.eia.gov/analysis/requests/ndaa/pdf/ndaa.pdf>.
- [33] "Finally: Phoenicia factory from Nazareth Illit is connected to the natural gas" ,*Globes*, February, 3, 2015 (in Hebrew). Retrieved: May, 2016, from <http://www.globes.co.il/news/article.aspx?did=1001006735>.
- [34] "Huge oil discovery on Golan Heights," *Globes* October, 7, 2015. Retrieved: May, 2016, from <http://www.globes.co.il/en/article-huge-oil-discovery-on-golan-heights-1001071698>.

A New Improvement of the Naturalistic Indicator of Forest Quality

An Italian Case Study

Silvia Assini

Dept. of Earth and Environment Sciences
University of Pavia
Pavia, Italy
Email: silviapaola.assini@unipv.it

Maria Grazia Albanesi

Dept. of Electrical, Computer and Biomedical Engineering
University of Pavia
Pavia, Italy
Email: mariagrazia.albanesi@unipv.it

Abstract— This paper describes a new improvement of the previous defined Forest Quality Indicator (FSQ) for biodiversity assessment and conservation purposes. The two novelties of the work in progress include the following aspects: the embedding of a shape feature of the forest patches, and the consideration of the plantation for ecological restoration in the computation of the indicator. The results are shown on a case study of a municipality of the West Po Plain (North Italy). The improved indicator seems to be very promising in describing the realistic situation of the forest quality in the territory. This suggests that it can be used efficiently to guide policy makers and planners to choose the best forest types/patches for restoration and connectivity.

Keywords - biodiversity; environmental indicator; forest status quality; patch shape; plantations.

I. INTRODUCTION

This work in progress represents a new improvement of the Naturalistic Indicator of the Forest Quality (Forest Quality Indicator, FSQ) described in [1]. Such indicator was performed considering the stratification, the percentage of alien species and the percentage of protected species (often corresponding to true forest species, such as *Anemone nemorosa*, *Campanula trachelium*, *Carex elongata*, *Convallaria majalis*, *Listera ovata*, *Neottia nidus-avis*, and *Primula vulgaris*) characterizing the different forest patches of the analyzed area (the Province of Pavia, Lombardy Region, North Italy). Furthermore, the proposed indicator took into account also the size of the forest patches, and only patches greater than 10.000 square meters were considered. In fact, patches smaller than 1 ha generally show low species richness [2] and a scarce floristic quality due to the edge effect which can increase the abundance of weedy and alien species [3]-[5]. The richness and floristic quality (due to true forest species) of the forest patches can be influenced not only by their size, but also by their shape. However, a correlation between the shape and the species richness of forest patches can be found when the patch size is sufficiently high. In fact, Dzwonko and Loster [6][7] found a negative correlation between the shape index of Patton [8] and the number of shrubs and forest species. In that case they worked with a restricted dataset of only 27 forests varying from 0.03 to 1.6 ha. With such small patch sizes it is possible that the entire patch was subject to the edge effects [9]. Honnay et al. [9] analyzed 234 forest

patches varying in size between 0.5 and 5216 ha and found a correlation between the Patton shape index and the number of species in edges and clearings, the number of woody species and lianas and, as a consequence, with the total number of forest plant species. For these reasons, in the new improvement of the FSQ indicator, also the shape of forest patches was taken into account. Patches with linear shapes were not considered, applying an *ad hoc* erosion operator on the image data provided by Geographic Information Systems (GIS) of the project (as explained in Section II.) Such linear patches, together with those smaller than 10.000 square meters, that can be considered as punctual patches, do not represent core areas hosting complexes forest ecosystems (as the wide patches of compact shape where the edge effect is reduced) important for woody and herbaceous true forest species. However, they can represent critical elements to connect core areas and support the structure of a local/regional ecological network, and the evaluation of their quality should be better considered from the connectivity perspective. Here, in the new improvement of the FSQ indicator, only forest patches with similar geometric characteristics (wide size and compact shape) were considered, with the aim to evaluate more homogenous elements and have a more realistic picture of the forest quality useful for conservation purposes.

Besides embedding the geometric characteristics in the computation of the FSQ indicator, a second aspect has been considered in this work in progress: the evaluation of the importance of forest plantations. In fact, in the previous elaboration of the FSQ indicator, only natural forests were considered, while plantations were excluded from the evaluation. However, the Lombardy Region, in 2002 started and financed an important project aimed to create 10 new plain forests, each of them with a size of about 40 ha and planted with native trees and shrubs [10][11]. Actually, such forests have not still developed a typical structure of mature wood and a typical nemoral herb layer, which will require at least 20-30 years. Anyway, because of their importance for the restoration of the Lombardy plain and conservation purposes, such new forests were considered in the present work in progress. The objective of the research is to analyze and quantify the impact of considering also the forest plantations (for restoration purposes) on the values of the FSQ. The case of the Municipality of Travacò Siccomario (Province of Pavia) was preliminary considered, to test this

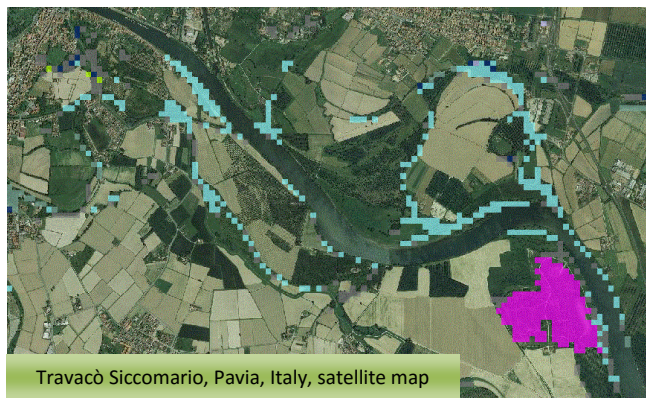


Figure 1. The territory under investigation (Municipality of Travacò Siccomario): the blocked colored areas superimposed on the geographic map show the presence of the natural forests (light green and light blue) and the plantation (pink).

elaboration because it hosts one of the ten new plain forests projected and realized with the support of Lombardy Region.

The aim of this paper is describing the data set and the methods used to extend the previous contribution in literature in the new work in progress. Moreover, to help readability, a brief summary on FSQ indicator is provided (for a detailed description, see [12].) The experimental results refer to the case study of the Municipality of Travacò Siccomario and they suggest an interesting starting point for future work.

II. DATA SET AND METHODS

As in the previous contribution [1][12], we have used a GIS database, free available from the Region Lombardy [13], in order to derive the useful description about the distribution of the forest in the territory. In Figure 1, the visual map for a portion of the Municipality of the case study under investigation is shown. Different colors refer to different types of forests. Particularly, the compact pink area refers to the forest plantation. The other colors refer to natural forests. These data are the input for both the two basic operations: the computation of the FSQ indicator (see Section II.A) and the processing by the Erosion operator (see Section II.B).

A. The Forest Status Quality Indicator

The FSQ expresses the forest quality status as the value of its ecological components, with particularly reference to the biodiversity conservation. In its first application [1][12] it was computed for each municipality of the provinces of Pavia and Lodi, considering only natural forests occurring on areas greater than 10.000 square meters [1]. A set of sub-regions occupied by natural forest F_i ($i = 1, 2, n$) was defined. Each of F_i may have one or more occurrences, denoted by the index k , in the territory ($k = 1, 2, \max(i)$). The number of occurrences may vary from a minimum of 1 to a maximum, which depends on the forest type ($\max(i)$). Each k -th occurrence is characterized by: (a) an area A_i^k ,

expressed in square meters, for $i = 1, 2, \dots, n$ and $k = 1, 2, \dots, \max(i)$, and (b) a type of T_i , derived from the GIS ERSAP Database “Map of the Forest Types of Lombardy” [13]. For each forest T_i , we found the correspondence with one or more phytosociological tables [14]. For each forest type T_i , we defined a set of the following indicator components (s_i, a_i, p_i): the stratification (number of layers) of a forest type i (s_i), the percentage frequency of alien species (a_i) in the corresponding phytosociological table/s, and the percentage frequency of protected species (p_i) (according to the Lombardy regional law, L.R. 10/2008) in the corresponding phytosociological table/s. The three components can assume only discrete values, from 0 to 3, according to an if – then – else algorithm described in [1][12]. After determining the values of the set of components for stratification, alien and protected species, for each forest T_i , it is possible to compute the FSQ Indicator of a municipality of area S as

$$FSQ = \sum_i \sum_k (s_i + a_i + p_i) * A_i^k / S \quad (1)$$

The FSQ definition is the weighted values of the components, where the weights are the ratios between the areas of the forests and the area of the territory under investigation. By using the primitives of the open source QGIS software [15], the values of A_i^k in the territory under investigation have been computed, in order to estimate the value of the FSQ indicator, according to (1).

B. The Erosion Operator

The first aspect of the work in progress here described is the introduction of the factor “shape” of the forest patches in the computation of the FSQ. By analyzing (1), in the original [1][12] FSQ definition, only the areas of forest patches are considered and weighted by the naturalistic components (s_i, a_i, p_i). The only limitation introduced on the geographic data is still a quantitative one (the 10.000 square meters as the minimum accepted size of the forest patch to be evaluated). However, we decided to take into consideration a characteristic that refers to the shape of a patch, i.e., to reduce the edge effect, which, in turn, reduces the floristic quality. This can be done by applying the standard mathematical morphology operator of Erosion [16], with a structural element of a circle of radius of 50 meters. In fact, Erosion is a typical image processing operator that allows to “erode” a connected area, starting from its perimeter and proceeding inside, of an extent that corresponds to a given shape of the structural element. In our case, the structural element is a circle of a given radius, in order to reduce the areas of the forests to their real inner shape, by excluding the areas near the boundary. If we use a circle as structural element, the shape of the forest will be remodeled in a symmetric way, all along the boundaries. The diameter of the structural element determines the minimum distance that a forest patch must have from its center to all the points of its boundaries, in order to be considered in the FSQ computation. As a result of the Erosion, the forest patches with a linear shape (a thin stripe less than 100 meters of amplitude) disappear from the map, as it can be seen in the

experimental results reported in Section III. All the other patches are reduced by the erosion, to minimize the “edge” effect. With the introduction of the Erosion operator, we applied to each area A_i^k the Erosion operator $E[\cdot]$, thus leading to a new expression of FSQ, denoted by FSQ_e :

$$FSQ_e = \sum_i \sum_k (s_i + a_i + p_i) * E[A_i^k] / S \quad (2)$$

The new operator FSQ_e takes into consideration both the quantitative (areas) and the qualitative (shapes) aspects of the forest patches.

C. The Study Area

The study area includes the Municipality of Travacò Siccomario (geographical coordinates: 45° 8' 60,00" N 9° 9' 38,52" E). It is located in the Lombardy plain at an average altitude above sea level of 66 meters, and is mainly characterized by agricultural fields and urban areas. Natural forest areas are localized along watercourses and channels, often as linear elements dominated by mixed woody species as *Salix alba*, *Populus alba*, *Quercus robur*, *Ulmus minor* and, very frequently, the invasive *Robinia pseudoacacia*. Wide forest patches are limited and dominated by the woody species above mentioned. As we consider only forest types that have at least one occurrence in the territory of area greater than 1 ha, only three types of natural forests survive these requirements: the *Salix alba* communities, the *Populus alba* communities, and *Robinia pseudoacacia* communities.

Moreover, in this study we want to include also plantations in the FSQ computation. In 2003-2004, one of the great plain forests of the Lombardy Region was realized in this municipality. Particularly meso-xerophilous and meso-igrophilous forest patches were realized on a surface of about 41 ha, planting native trees (such *Populus nigra*, *Ulmus minor*, *Acer campestre*, *Malus sylvestris*, *Carpinus betulus*, *Quercus robur*, *Salix alba*, *Alnus glutinosa*, *Populus alba*, *Prunus padus*) and native shrubs (such *Crataegus monogyna*, *Corylus avellana*, *Prunus spinosa*, *Sambucus nigra*, *Cornus sanguinea*, *Frangula alnus*, *Viburnum opulus*, *Salix cinerea*). Considering the woody floristic composition, the new forest can be considered as the forest type Oak-Elm wood (also including the Black Alder variant) [17]. The value set of components for stratification, alien and protected species is 3,2,2 for this plantation. In Table I all the forest types, of area greater than 1 ha, for the case study of Travacò Siccomario are shown.

III. EXPERIMENTAL RESULTS

In the experiments of data analysis, for the case study here reported, we applied the erosion operator to compute the FSQ_e , according to (2) and compare the effect of the Erosion on each forest types of Table I. The computed value FSQ_e for the Municipality of Travacò Siccomario is 0.2004, vs. a value of FSQ of 0.2276, including all the forest types of Table I (both natural forest and plantation). The relative loss of the indicator is of 11.9%.

TABLE I. FOREST TYPES FOR THE CASE STUDY.

Naturalistic components (s_i, a_i, p_i) .	Description of forest types T_i and relative reference <i>syntaxa</i>
(1,1,0)	T_1 : Willow wood of bank
(3,1,0)	T_2 : White Poplar formation
(2,1,0)	T_3 : Pure <i>Robinia pseudoacacia</i> wood
(3,2,2)	T_4 : Plantation (Oak-Elm wood, also including the Black Alder variant)



Figure 2. The territory under investigation after the Erosion operator applied to all the forest patches.

Clearly, the erosion has reduced the areas of the forest patch, and consequently the indicator is lower. However, the loss of the areas is not equal for all the four forest types. In fact, the loss is determined by the shapes of the patches, which are quite different in the territory under examination. The loss percentages are the following: 3.6% for the plantation, 35.2% for the *Salix alba* communities, 51.3% for the *Populus alba* communities, and 61.2% for the *Robinia pseudoacacia* communities. It is interesting to note that the plantation is the forest type with the lowest loss; this indicates that the project has considered a good shape, which is very close to an ideal core area. Moreover, the *Robinia pseudoacacia* communities have the highest loss, and it is a positive aspect, because of the very low floristic quality, due to the dominance of alien species in linear and fragmented patches. In Figure 2, the map of the territory after the erosion is shown. The reduction of the colored areas of the forests types is evident, by comparing Figure 2 to Figure 1. In Figure 3, the areas before and after the erosion are plot, for each forest type of Table I.

IV. CONCLUSION AND FUTURE WORK

The new improvement of the FSQ here presented and the obtained experimental results put in evidence that our methodological approach is realistic in evaluating the forest quality and may give useful information for the choice of which forest patches should be enhanced for conservation purposes (in our case study, *Salix alba* and *Populus alba* communities) or not (*Robinia pseudoacacia* communities). The promising results suggest to extend the FSQ_e computation for all the municipalities considered in [12].

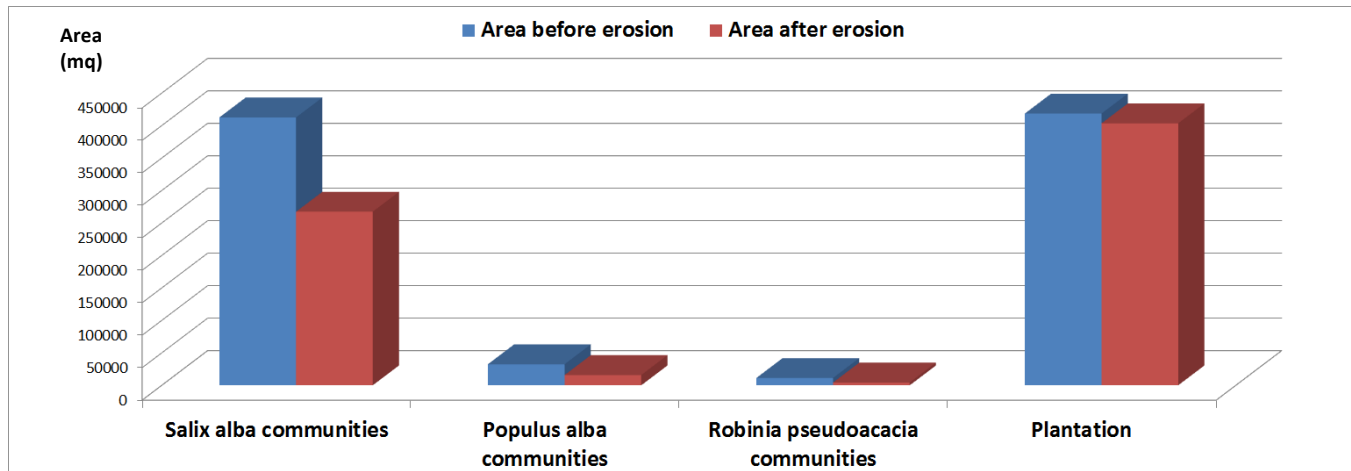


Figure 3. The areas (in square meters, on Y-axis) for each the forest types (on the X-axis), before and after the Erosion.

REFERENCES

- [1] S. Assini and M. G. Albanesi, "A Naturalistic Indicator of the Forest Quality and its Relationship with the Land Use Anthropentropy Factor," Proceedings of the Sixth International Conference on Bioenvironment, Biodiversity and Renewable Energies (BIONATURE 2015), Rome (Italy), 24-29 May 2015, Copyright (©) IARIA, 2015, pp. 27-33, ISBN 978-1-61208-410-7.
- [2] P. Digiovinazzo, G. F. Ficetola, L. Bottoni, C. Andreis, and E. Padoa-Schioppa, "Ecological thresholds in herb communities for the management of suburban fragmented forests," *Forest Ecology and Management*, vol. 259, 2010, pp. 343-349.
- [3] D. A. Saunders, R. J. Hobbs, and C. R. Margules, "Biological consequences of ecosystem fragmentation: a review," *Conservation Biology*, vol. 5, 1991, pp. 18-32.
- [4] O. Honnay, K. Verheyen, and M. Hermy, "Permeability of ancient forest edges for weedy plant species invasion," *Forest Ecology and Management*, vol.161, 2002, pp.109-122.
- [5] W. F. Laurance et al., "Ecosystem decay of Amazon forest fragments: a 22-year investigation," *Conservation Biology*, vol. 16, 2002, pp. 605-618.
- [6] Z. Dzwonko and S. Loster, "Species richness of small woodlands on the western Carpathians foothills," *Vegetatio*, vol. 76, 1988, pp. 15-27.
- [7] Z. Dzwonko and S. Loster, "Species richness and seed dispersal to secondary woods in southern Poland," *Journal of Biogeography*, vol. 19, 1992, pp. 195-204.
- [8] D. R. Patton, "A diversity index for quantifying habitat edge," *Wildlife Society Bulletin*, vol. 3, 1975, pp. 171-173.
- [9] O. Honnay, M. Hermy, and P. Coppin, "Effects of area, age and diversity of forest patches in Belgium on plant species richness, and implication for conservation and restoration," *Biological Conservation*, vol. 87, 1999, pp. 73-84.
- [10] F. Sartori and S. Assini, "First evaluation of the regional afforestation actions of the lombardy plain", Transl. "Prime valutazioni sulle opere regionali di riforestazione della pinaura lombarda", «NATURA BRESCIANA» Ann. Mus. Civ. Sc. Nat., Brescia, 36, 2009, pp. 191-196.
- [11] S. Assini and F. Sartori, "Vegetation and restoration – Monitoring of the actions: the great plain forests of the Lombardy Region. Analyses and perspectives", Transl. "Vegetazione e riqualificazione – Monitoraggio degli interventi: le grandi foreste di pianura della Regione Lombardia. Analisi e prospettive", Quaderni di Tutela del Territorio, Regione Piemonte, 3, pp. 57-65, 2009.
- [12] S. Assini and M.G. Albanesi, "A New Biodiversity Composite Indicator Based on Anthropentropy and Forest Quality Assessment. Framework, Theory, and Case Studies of Italian Territory", *IARIA International Journal On Advances in Life Science*, 7 (3-4), 2015, pp. 177-194.
- [13] Regional Organization for Services in Agriculture and Forests, Transl. Ente Regionale Servizi Agricoltura e Foreste, "Map of Forest Types of Lombardia", Transl. "Carta dei tipi reali forestali della Lombardia," <http://www.geoportale.regione.lombardia.it/galleria-mappe>, page 3 [retrieved: May, 2016].
- [14] C. Andreis and F. Sartori, eds, "Forest vegetation of Lombardia. Phytosociological classification," Transl. "Vegetazione forestale della Lombardia. Inquadramento fitosociologico," *Archivio Geobotanico*, vol. 12-13, 2011, pp. 1-215.
- [15] QuantumGIS software, <http://www.qgis.org/en/site/> [retrieved: May, 2016].
- [16] R. C. Gonzales and R. E. Woods, *Digital image processing*, Pearson Prentice Hall, 2008, Chapter 9, "Morphological image processing".
- [17] R. del Favero, ed., "The forest types of Lombardy", Transl. "I tipi forestale della Lombardia", CIERRE Edizioni, pp. 506, 2002.

The Assessment of Environmental Changes of Selected Water Bodies in the Area of Cracow over the Past Two Decades

Peter Eggenbauer

Master's Programme Industrial Environmental Protection
and Process Technology
Montan University, Leoben, Austria
e-mail: peter_eggenbauer@hotmail.com

Boris Tokmačija

Faculty of Science and Education
University of Mostar
Mostar, Bosnia and Herzegovina
e-mail: silver-toki@hotmail.com

Aleksandra Obrist

University of Basel
Basel, Switzerland
e-mail: a.obrist@stud.unibas.ch

Aleksandra Wagner*

Dept. Geoinf., Photogrammetry & Remote Sensing of Env.
AGH University of Science and Technology
Kraków, Poland
e-mail: awagner@agh.edu.pl

Abstract—Six water bodies or their complexes - four in Cracow and two in the Commune of Niepołomice, Southern Poland - were studied focusing the changes they have undergone and the present state from the point of view of their attractiveness to the visitors. The degree of threat to the water bodies was also assessed. The highest grades were given to the ponds of Niepołomice (Zamkowa), due its well management. The lowest grades were attributed the ponds of Płaszów (also the most threatened pond) and Staniątki (probably a temporary situation). The least threatened complex of water bodies is the one in Przylasek Rusiecki. Two of the described water bodies (Dąbie and Staniątki) diminished their area within the last 20 years and the pond of Płaszów diminished earlier.

Keywords - water bodies; tourism; chemical analysis; sustainable development.

I. INTRODUCTION

Small and medium size water bodies are habitats often subdued to various changes, related both to weather/climate fluctuations as well as direct human influence [1]-[5]. They can be subdued to drainage as much as polluting factors much easier than bigger water bodies. The region of Cracow (in Polish Kraków) is rich in small water bodies [3]-[5]. Many of them are human made [5], [6]. Over their longer or shorter history they went through different changes in their functions and the function of the ecosystems surrounding them. One of the important function, apart from small retention and ecological function is recreational function. This function depends on the natural properties of the water body (size, shape of the shoreline) and the way of management (facilities, maintenance of the area, etc.) [5]-[8]. Another important function is maintaining biodiversity. Water bodies attract animals and plants, including rare species. This creates opportunities for nature-based tourism and increase tourist attractiveness.

There are two main objectives of this paper: (1) to present changes in selected water bodies of Cracow over the

last two decades and, if possible, also earlier and (2) to quantify the assessment of the sites from the point of view of sustainable development. The assessed values were tourist attractiveness, understood as the amount of features that could be attractive to visitors from the point of view of leisure and/or sight-seeing (including observations of fauna and flora), as well the degree of threat, understood as quantified expression of various dangers to the water body. It does not necessarily have to be the threat of total disappearance of the water body, but also all the factors making the water body or its surroundings less attractive or diminishing the biodiversity of the area. Section II briefly describes the study area. Section III presents the methods of the studies. Section IV presents the results of long term observations and laboratory analyses. In Section V proposals of changes are discussed in the context of social responsibility.

II. THE STUDY AREA

The water bodies in two communes – the city of Cracow and the commune of Niepołomice (Wieliczka District) were studied. The selection included water bodies of anthropogenic origin. They were the following:

Ponds situated in the city of Cracow:

1. Staw Płaszowski (the Płaszów Pond) - a 9.0 ha borrow pit formed after the exploitation of sand and gravel in 1930s. The area of the pond was decreased. In 1975 and 1965 it had a surface of 9.98 ha and 11.95ha, respectively [6]. The diminishing of the surface was due to making an open market and then covered market.
2. Bagry – a borrow pit of 30.1 ha, also formed in 1930s. Used as bathing resort. Its surface did not change much. The infrastructure has been improving over the years.
3. Staw Dąbski (the Dąbie Pond, 2.1 ha – situated in Craców, east from the centre, formed in 1930s after the exploitation of clay. Originally, there were more ponds,

but in 1960s they were filled in and only one remained. The original area of 2.6 ha has been diminished due to the building of the Market and Entertainment Centre (*Centrum Handlowo-Rozrywkowe*) "Plaza" [6]. In 2010 the pond was announced Environmentally Useful Area by the City Council of Cracow [9].

4. Przulasek Rusiecki – a complex of 10-11 gravel borrow pits (the number is changeable, because some water bodies can temporarily be joint or separated), of the total area of 82.19 ha, situated in the eastern part of Cracow, quarter Nowa Huta. One of the ponds makes bathing resort.

5. Niepołomice – Zamkowa street - 0.1 ha. The pond undergone restoration works in 2005. The shores were reinforced with wicker and an islet was formed in the middle. However, after a few years the islet submerged. Significant changes in the surroundings were also observed. The pond was originally an anti-fire reservoir and fishing pond. Nowadays fishing is forbidden and the pond has a decorative function, as a part of the local ethnographic museum [5]. Some changes were illustrated in the photographs in Figure 1.

6. Staniatki (the Commune of Niepołomice), Figure 6. – two ponds near the Benedictine Convent in Zagórska street, 0.12 and 0.05 ha. Originally, it was one pond, with a bigger surface. It served as a fishing pond. Later on it was abandoned, but in 1996 the project of management was accepted. In 2005 facilities such as a railing and teeters were built. They were destroyed due to the construction works regarding the neighbouring buildings [5]. Changes were illustrated in the photographs in Figure 1.

Information about locations is contained in [5]-[8].

III. METHODS

The following methods were applied:

A. Field Observations and Area Measurement

Study visits were carried out in every location. The observations of fauna and flora were made. The area of the water bodies was measured based on airborne images received from the Polish Central Geodetic and Cartographic Resource and calculated by the Quantum GIS program.

B. Laboratory Analyses

Laboratory analyses were carried out in October and November 2015, at AGH University of Science and Technology in Cracow, Faculty of Mining Surveying and Environmental Engineering, Laboratory of Department of Environmental Management and Protection, led by Ms. Marta Nowak-Bator, M.Sc., Eng. The instrument for the measurements was photometer PF-12, by AQUA Lab. If possible, the results were compared to the earlier results of analyses.

C. Semi-quantitative Assessment

To assess the value (tourist attractiveness) of each water body and the way it is threatened, the Saaty method of hierarchic analysis [10] was applied to give weight to each characteristic (parameter). Namely, the authors had to decide, which feature is more and which less important. The weights were calculated in such a way that the characteristics were compared in pairs and for each pair the decision was made in terms of which characteristic was more important. The following intensities of importance, for each pair, were considered: 1 – equal importance, 3 – moderate importance, 5 – importance, 7 – very strong importance, 9 – extreme importance. Less important characteristics of the less important value of each pair took values: 1/3, 1/5, 1/7, 1/9, respectively. The calculations were made using the computer programme by K. D. Goepel [11]. The values of weights are shown in Tables I and II. For each characteristic, grade 1-4 was given (4 was the highest). All the characteristics contribute to the value of tourist attractiveness (leisure and sightseeing opportunities) or the degree of threat. Finally the following formula was applied:

$$S = \sum_{i=1}^n w_i x_i$$

where:

S – final assessment

x_i – assessment of subsequent parameters

w_i – weights of subsequent parameters

.

The parameters (characteristics) were the following:

- 1) *Facilities*: benches, sanitary facilities, restaurants, etc.
- 2) *Flora and Fauna* – species protected by law, especially included in the EU Directives
- 3) *Sports and leisure* – swimming, playgrounds etc.
- 4) *Water* – derived from laboratory analyses
- 5) *Landmarks* – points important from historical or cultural point of view
- 6) *Landscape* – the easthetic impression about landscape
- 7) *Management* – is the area clean and tidy?

The degree of threat to the water bodies was also assessed and computed as a sum the following characteristics:

- 1) *Landscape degradation* – visual degradation
- 2) *Transport* – the proximity to the road
- 3) *Drainage or backfilling* – to which extent it occurred
- 4) *Industry* – the proximity of industrial plants
- 5) *Vandalism and littering* – amount of litter and damage
- 6) *Invasion of alien species* – number of alien plant species, based on observation and previous studies [6]

The criteria were based on previous papers [3] and [8], but modified, according to the specifics of this study.

TABLE I THE WAY OF CALCULATING WEIGHTS REFERRING TO VARIOUS ASPECTS OF TOURIST ATTRACTIVENESS

	F	FF	SL	W	LM	LS	M	Weight
Facilities	1							0.217
Flora and Fauna	1	1						0.132
Sports & Leisure	1	1	1					0.137
Water	1	1	3	1				0.190
Landmarks	1/3	1	1	1	1			0.139
Landscape	1/3	1	1/3	1/3	1	1		0.084
Management	1/3	1	1	1	1/3	1	1	0.100

TABLE II THE WAY OF CALCULATING THREAT REFERRING TO VARIOUS ASPECTS OF THREAT TO WATER BODIES

	L	T	D	I	V	A	Weight
Landscape degradation	1						0.077
Transport	3	1					0.238
Drainage or backfilling	1	1	1				0.185
Industry	3	1	3	1			0.294
Vandalism and littering	3	1/3	1/3	1/3	1		0.103
Alien species	3	1/3	1/3	1/3	1	1	0.103

IV. RESULTS

The results of laboratory analyses are shown in tables III and IV. The values were compared to the Enactment of the Minister of Environment [12]. The Figures in bold mean the values exceeding the maximum accepted values for the first and second class of the water quality in the mentioned Enactment. For the conductivity this value is given in Enclosure II (values for lakes and reservoirs) and both for first and second class must not exceed $\mu\text{S}/\text{cm}$. For other values, which are not included in the Enclosure II, values in Enclosure I (for rivers and streams) were taken. In most cases there was no visible trend in time referring to the parameters. There were no bigger changes in pH, which ranged from 7.0 (Niepołomice) to 8.9 (Przylasek Rusiecki). Conductivity was the parameter which was exceeded in most of the locations. The highest value was in Dąbie in 2008. In 2015 the value was lower, nevertheless remained high. In all the locations conductivity values of 2015 were lower than in 2008. Chemical analyses showed that the values of nitrates were high only in Niepołomice and the highest values of phosphates were in Dąbie (in 2003 and 2008). The values of chlorides were low, except of Płaszów.

The analyses of the airborne images and personal observations show that over the last 20 years the area of the Dąbie Pond and the Staniątki Pond decreased in 1990s and the area of the Płaszów pond decreased in 1960s and 1970s.

Observation of animals focused on birds, because they have the greatest significance for amateur nature observations (bird watchers). The list of animals observed in the ponds is given in table V. Species included in the Bird Directive and Habitat Directive (Enclosure 1) are marked with letters P and D, respectively. The bird included into the Bird Directive was the common tern *Sterna hirundo*, seen on the Bagry pond.

The management of the area changed most in Dąbie, Niepołomice and Staniątki (still undergoing changes).

Table VI shows the values and grades attributed to each site, according to the method described in Section III. The

highest grade can be given to the pond of Niepołomice, especially due to very good management. The second grade is given to Bagry. The Pond of Dąbie received 3rd grade. The maximum assessment of the flora and fauna is not due to birds, but due to the presence of the Amur bitterling *Rhodeus sericeus* (Pallas) [13]. The lowest values were received by the ponds of Płaszów and Staniątki. In the latter case, the area was under construction.

The most threatened pond is the pond of Płaszów. The biggest problem there is littering and (to certain extent) vandalism. The area is being built up and the pond is not the object of interest of the public, so it is subdued to degradation. On the second place is the pond of Staniątki, nevertheless the present state seems to be temporary. The least endangered is the complex of ponds in Przylasek Rusiecki.

V. CONCLUSIONS

The study showed that the water bodies of Dąbie, Staniątki and Staniątki were undergoing big changes, especially in the state of management. Unfortunately one can fear that if the area is "too well managed" (reed regularly cut) the habitat for the birds nesting in the reed (e.g., moorhen) will be destroyed.

The water bodies of Dąbie and Staniątki diminished their area within the last 20 years and the pond of Płaszów diminished in 1960s and 1970s. Other ponds did not change much in surface, but there were changes in the management of the surrounding area.

In the commune of Niepołomice (ponds of Niepołomice and Staniątki), the biggest improvement in the aesthetics of the area was carried out in 2005. Some of these changes were not long lasting, though.

The highest differences in the assessment of water bodies were observed in the facilities provided and the management. The smallest differences were referring to landscape.

The water bodies can contribute to sustainable tourism as well as economic development of the area. Nevertheless, in some cases (Płaszów, Staniątki) their potential is not fully used. The improvement in the management is highly recommended. This should include cleaning as well as putting information tables about the flora and fauna.

ACKNOWLEDGMENT

The authors wish to thank Ms. Marta Nowak-Bator, M.Sc., eng. and Dr Zbigniew Kowalewski, Eng. for their help in carrying out the laboratory analyses. The paper was supported by the grant Badania Statutowe AGH no. 11.11.150.949 /16. The paper was done within the IAESTE exchange programme.

REFERENCES

- [1] "Small water bodies - Assessment of status and threats of standing small water bodies, version: 1.1. ETC/Water task.milestone.submilestone: Task 8, EEA Project manager: N. Thyssen, 2009. [Online] http://icm.eionet.europa.eu/ETC_Reports/Assessment%20of%20status%20and%20threat%20of%20standing%20small%20water%20bodies.pdf 2016.05.30.

- [2] P. Pieńkowski, P., 2003. Disappearance of the mid-field ponds as a result of agriculture intensification. *Journal of Polish Agricultural Universities* 6:2.
- [3] E. Panek and D. Bedla, "Ecological and landscape valuation of small water bodies in the selected municipalities of the Małopolska Province", and *Environmental Engineering* (previous title: *Geodezja oraz Inżynieria Środowiska*) 2, 4, pp. 58-68, 2008
- [4] E. Panek and B. Rajpolt, "Preliminary studies on the protecting possibilities of selected small water bodies in the area of Krakow agglomeration", *Geomatics and Environmental Engineering* (previous title: *Geodezja oraz Inżynieria Środowiska*) 7, 2, pp. 45-59, 2013
- [5] A. Wagner "Valuation of water bodies in the Krakow region for the needs of the concept of management according to the principle of sustainable development" [Waloryzacja zbiorników wodnych w rejonie Krakowa dla potrzeb opracowania koncepcji ich zagospodarowania, zgodnie z zasadami zrównoważonego rozwoju] – manuscript, unpublished.
- [6] A. Wagner and D. Hruševar, "Contribution to the Knowledge of Plant Diversity in the Małopolska Region. Focus on Invasive Plants in Kraków and Vicinity," *International Journal On Advances in Life Sciences* 7, 3/4, pp. 158-176, 2015
- [7] M. Orlewicz-Musiał and A. Wagner "Transformations of urban green areas related to the development of sports and recreational infrastructure; focus on the area of Nowa Huta in Krakow" [Przeobrażenia terenów zieleni miejskiej w związku z rozwojem infrastruktury sportowo-rekreacyjnej na przykładzie dzielnic Nowej Huty w Krakowie], In: *Kierunki zmian terenów zieleni w miastach*, ed. M. Kosmala, Toruń, PZiITS, pp. 241-252, 2014.
- [8] A. Wagner and D. Hasanagić, "Comparative analysis of selected water bodies in Cracow and vicinity in terms of their revitalization," *Innowacyjne rozwiązania rewitalizacji terenów zdegradowanych* [Innovative solutions of the revitalization of degraded areas] (ed. J. Skowronek) Instytut Ekologii Terenów Uprzemysłowionych; Centrum Badań i Dozoru Górnictwa Podziemnego Sp. z o. o., pp. 139-152, 2014.
- [9] "Resolution no. XC/1202/10 of the City Council of Krakow of 13th January 2010 on Establishing the Ecologically Useful Area "The Pond of Dąbie"" [Uchwała nr XC/1202/10 XC/1202/10 Rady Miasta Krakowa z dnia 13 stycznia 2010 r. w sprawie ustanowienia użytku ekologicznego "Staw Dąbski"], [Online]. Available from: <http://www.infor.pl/akt-prawny/U80.2010.045.0000302,uchwala-nr-xc120210-rady-miasta-krakowa-w-sprawie-ustanowienia-uzytku-ekologicznego-staw-dabski.html> 2016.03.01.
- [10] T. L. Saaty, "The Analytic Hierarchy Process: Planning, Priority Setting", Resource Allocation. McGraw-Hill, 1980.
- [11] K. D. Goepel, "Concepts, Methods and Tools to manage Business Performance" [Online]. Available from: <http://bpmmsg.com/> 2016.03.01.
- [12] "The Enactment of the Minister of Environment of 22nd October 2014 on the way of classification of the state of surface water bodies and environmental standards of quality for the priority substances" [Rozporządzenie Ministra Środowiska z dnia 22 października 2014 r. w sprawie sposobu klasyfikacji stanu jednolitych części wód powierzchniowych oraz środowiskowych norm jakości dla substancji priorytetowych]. *Dziennik Ustaw*, position 1482, 2014.
- [13] B. Szczęsny et al., "The Dąbie Pond. Reports of the first stage of ecological studies of the Dąbie Pond done in 2003 on the request of the 'Foundation Partnership for the Environment'" [Staw Dąbski. Sprawozdania I etapu badań ekologicznych „Stawu Dąbskiego” wykonanych w 2003 r. na zlecenie „Fundacji Partnerstwo dla Środowiska”]. Kraków, Instytut Ochrony Przyrody PAN, 2003, unpublished.

TABLE III. PHYSICAL AND CHEMICAL PARAMETERS OF WATERS IN THE WATER BODIES NEAR IN CRACOW AND VICINITY

Location	pH								Conductivity [µS/cm]							
	1996-1997	1998	1999	2001-2004	2005	2008	2015 ⁶	2015 ⁷	1996	1999	2002-2004	2005	2008	2015 ⁶	2015 ⁷	
Płaszów	Not measured			8.1 ¹		8.4	7.8	n.m.	n.m.		1600 ¹	n.m.	1417	1166	n.m.	
Bagry - west	Not measured			8.2 ²	8.6	7.8	8.4	n.m.	Not measured				2250	585.5	n.m.	
Bagry - east	Not measured			n.m.	8.5	7.7	8.0	n.m.	Not measured			717	1426	622.6	n.m.	
Dąbie	Not measured			7.6 ³		7.7	8.3	n.m.	Not measured		1291 ³	n.m.	2336	1094.5	n.m.	
Przylasek - road	Not measured							7.7	7.6	n.m.					409.5	373.5
Przylasek - beach	8.7 ³	n.m.	8.2	7.8 ⁴	8.3	8.9	7.9	7.6	n.m.	610	422 ⁴	574	958	402.5	429.5	
Niepołomice	7.0 ⁵	7.0	7.0	7.3 ⁴	8.1	n.m.	7.9	n.m.	990 ⁵	680	591 ⁴	740	n.m.	733.5	n.m.	
Staniątki	7.5 ⁵	7.1	7.5	n.m.	7.3	n.m.	7.7	n.m.	800	133	762 ⁴	n.m.		544.5	n.m.	

¹Measurements made on 25/07/2001; ²Measurements made on 1/05/2004; ³Mean of two measurements taken on 24/09/2003 by Szczęsny et al. [11], ³Measurements made on 19/08/1997, ⁴Measurements made in 2002, ⁵Measurements made in 1996, ⁶Mean of two measurements on 5/10/2015; ⁷ Mean of two measurements on 21/10/2015

TABLE IV. PHYSICAL AND CHEMICAL PARAMETERS OF WATERS IN THE WATER BODIES IN CRACOW AND VICINITY

Location	NO ₃ ⁻		PO ₄ ³⁻ [mg/dm ³]				Cl ⁻				
	2015 ⁶	2015 ⁷	2003	15/10/2008	2015 ⁶	2015 ⁷	1996	1997	1999	2015 ⁶	2015 ⁷
Płaszów Pond	0.7	n.m.	n.m.	0.349	0.20	n.m.	Not measured			241.4	n.m.
Bagry - Łanowa	0.0	n.m.	n.m.	n.m.	0.215	n.m.	Not measured			56.8	n.m.
Bagry - Bagrowa	0.0	n.m.	n.m.	1.095	0.155	n.m.	Not measured			56.8	n.m.
Dąbie	0.0	n.m.	1.2665	1.095	0.38	n.m.	Not measured			110.05	n.m.
Przylasek - road	0.25	<1.0	n.m.	n.m.	0.31	0.20	Not measured			56.8	60.35
Przylasek - beach	0.1	<1.0	n.m.	n.m.	0.185	0.85	Not measured			56.8	56.8
Niepołomice	7.35	n.m.	n.m.	n.m.	0.25	n.m.	82.4	50.00	54	127.8	n.m.
Staniątki	1.25	n.m.	n.m.	n.m.	<0.2	n.m.	40.7	n.m.	42	35.5	n.m.

TABLE V. BIRDS OBSERVED AT THE WATER BODIES IN CRACOW AND VICINITY

Location	Płaszów	Bagry	Dąbie	Przylasek	Niepołomice	Staniątki
Mute Swan <i>Cygnus olor</i> (Gmell.) ^P	+++	+++	+++	+		
Mallard <i>Anas platyrhynchos</i> L.	+++	+++	+++	+++	+++	++
Tufted Duck <i>Aythya fuligula</i> (L.)				+ (April 2003)		
Coot <i>Fulica atra</i> (L.)	+++	+++	++			
Moorhen <i>Gallinula chloropus</i> (L.) ^P						+ (April 1996)
Great Crested Grebe <i>Podiceps cristatus</i> ^P	++	++	+ (April 2007)	++		
Common Gull <i>Larus canus</i> L. ^P				++		
European Herring Gull <i>Larus argentatus</i> L. ^P				++		
Black Headed Gull <i>Larus ridibundus</i> L. ^P	+++	+++	+++	++		
Common Tern <i>Sterna hirundo</i> L. ^D		++				
Great Cormorant <i>Phalacrocorax carbo</i> (L.) ^P		++		+++		
Barn Swallow <i>Hirundo rustica</i> L. ^P		++		++		
House Martin <i>Delichon urbica</i> (L.) ^P					++	

^P – species protected by the Polish Law, ^D – species included in the Enclosure 1 of Bird Directive

+++ observations of October 2016

++ only observations before October 2016 (more than once)

+ only one observation

TABLE VI. ASSESSMENT OF WATER BODIES IN CRACOW AND VICINITY

Location	Facilities		Flora and Fauna		Sports and leisure		Water		Landmarks		Landscape		Management		Total Assessment and Rank	
	A	B 0.217	A	B 0.132	A	B 0.137	A	B 0.190	A	B 0.139	A	B 0.084	A	B 0.100	Without weight	With weight
Płaszów	3	0.651	3	0.396	2	0.274	2	0.380	2	0.278	2	0.168	1	0.100	15 (6)	2.247 (5)
Bagry	4	0.868	3	0.396	3	0.411	3	0.570	2	0.278	2	0.168	3	0.300	20 (2)	2.991 (2)
Dąbie	4	0.868	4	0.528	2	0.28	2	0.380	2	0.278	2	0.168	4	0.400	20 (2)	2.902 (3)
Przylasek	2	0.434	3	0.396	3	0.411	3	0.570	2	0.278	3	0.252	2	0.200	18 (4)	2.541 (4)
Niepołomice	4	0.868	2	0.264	2	0.274	2	0.380	4	0.556	3	0.252	4	0.400	21 (1)	2.994 (1)
Staniątki	1	0.217	2	0.264	1	0.137	3	0.570	4	0.556	2	0.168	3	0.300	16 (5)	2.212 (6)

A – the assessment in 1-4 scale, B – with weight; ranks given below

TABLE VII. ASSESSMENT OF THE THREAT TO THE WATER BODIES IN CRACOW AND VICINITY (explanations like in table VI)

Location	Landscape degradation		Transport		Drainage or backfilling		Industry		Vandalism and littering		Invasion of alien species		Total Assessment and Rank	
	A	B 0.077	A	B 0.238	A	B 0.185	A	B 0.294	A	B 0.103	A	B 0.103	Without weight	With weight
Płaszów	2	0.154	3	0.714	1	0.185	3	0.882	4	0.412	3	0.309	16 (1)	2.656 (1)
Bagry	3	0.231	2	0.476	1	0.185	3	0.882	2	0.206	2	0.206	13 (4)	2.186 (5)
Dąbie	2	0.154	3	0.714	2	0.370	3	0.882	1	0.103	2	0.206	13 (4)	2.429 (3)
Przyłasek	2	0.154	2	0.476	1	0.185	2	0.588	2	0.206	2	0.206	11 (6)	1.815 (6)
Niepołomice	3	0.231	3	0.714	3	0.555	1	0.294	2	0.206	2	0.206	14 (3)	2.206 (4)
Staniątki	2	0.154	3	0.714	4	0.740	2	0.588	2	0.206	2	0.206	15 (2)	2.608 (2)



Figure. 1. The pond in Niepołomice. Left: April 1996 – view from the eastern side (Zamkowa Street); centre: July 2005 – view from the western side (3Maja Street), the pond after the renovation works – the islet is visible; right: October 2015 – the islet is appeared, the note saying that fishing is forbidden was put. Previously the pond was used for fishing, photos: A. Wagner.



Figure 2. The fragment of the Staniątki Pond. Left: 2nd May 1996; centre: 1st August 2005 – the railing was built; right: 10th November 2015 – the white building on the left is the newly built nursing home, the railing was removed, photos: A. Wagner.

Analysing the fAPAR Dynamic Over Europe Using MODIS Data

Carmelo Cammalleri, Fabio Micale, Jürgen Vogt

European Commission, Joint Research Centre (JRC)

21027 Ispra (VA), Italy

e-mails: carmelo.cammalleri@jrc.ec.europa.eu; fabio.micale@jrc.ec.europa.eu; juergen.vogt@jrc.ec.europa.eu.

Abstract—This paper analyses the temporal dynamic of long-term fraction of Absorbed Photosynthetically Active Radiation (fAPAR) time series over Europe as derived from a 15 years dataset of satellite images collected between 2001 and 2015 from the Moderate-Resolution Imaging Spectroradiometer (MODIS) sensor onboard of Terra satellite. A fitting of piecewise logistic functions of time was performed for each cell in order to account for the multi-cycle dynamic of fAPAR. Most of the cells within the domain area showed a single peak cycle, even if a non-negligible fraction of the domain (about 15%) showed two distinct peaks in the yearly cycle. The results of the logistic function fittings allow identifying the key transition dates between increasing/decreasing trends in fAPAR, constituting a starting point for a more detailed analysis of drought effects on ecosystems.

Keywords- fAPAR; vegetation cycle; EDO; MODIS.

I. INTRODUCTION

The understanding of the phenological cycle of land ecosystems is a key element in the analysis of the feedbacks between climate and Earth's biosphere. The fraction of Absorbed Photosynthetically Active Radiation (fAPAR) has been widely identified as a suitable proxy of the greenness and health status of vegetation, thanks to its central role in both plant primary productivity and carbon dioxide absorption. The Global Climate Observing System (GCOS) recognized fAPAR as one of the 50 climate variables essential to characterize the climate of the Earth [1].

The spatiotemporal variability of fAPAR can be derived from space by means of the inverse solution of the radiation transfer through the canopy space. Several remote sensing based fAPAR products are currently available, including the ones from the Advanced Very High Resolution Radiometer (AVHRR), the Moderate-Resolution Imaging Spectroradiometer (MODIS) and the PROBA-V; particularly, the MODIS standard product MOD15A2 is characterized by a relatively long time series (starting in 2000) and a near real time update.

The observed sensitivity of fAPAR to vegetation stress has suggested its use in drought monitoring [2] [3]; an example is the role of fAPAR anomalies in the Combined Drought Indicator (CDI) developed for agricultural drought monitoring in the European Drought Observatory (EDO) [4] [5].

Even if the simple fAPAR anomalies have proven to be reliable for drought detection [6], the fAPAR response to drought may vary as a function of the timing and

phenological phase (i.e., early stage, late growth) [7], this latter characterized by a temporal variability influenced by climate change [8]. Generally, it seems valuable to quantify the capability to automatically identify the phenological stage at which a certain fAPAR anomaly occurs.

Several methodologies have been proposed in the past to capture the timing of key phenological phases in remote sensing fAPAR time series, including fixed thresholds [9], moving averages [10], lagged moving average [11], Fast Fourier and Harmonic Analysis [12], and fitting of smooth functions [13] [14], as well as to evaluate the impact of climate and used datasets on key transition dates [8] [15].

In this paper, we test the use of a series of piecewise logistic functions to fit a time series of fAPAR images collected by the MODIS-Terra sensor over Europe in the period 2001-2015. Advantage of logistic function is the capability to reproduce the succession of relatively constant low and high values linked by transition periods, as observed in most fAPAR records.

Goal of the study is to identify the suitability of the methodology to detect the key transition dates for a future integration of this approach in an operational drought monitoring system like EDO. In Section II, the processing of satellite data and the mathematical background of the fitting procedure are described, in Section III the main results of the fitting, including the detected number of peaks and the key transition dates, are detailed, and, finally, in Section IV a summary of the results is reported, as well as some key conclusions of the study are illustrated.

II. MATERIALS AND METHODS

In this Section, the pre-processing of the remotely sensed data, as well as the procedure to derive the key transition dates, are described in details.

A. Satellite fAPAR data

Physically based fAPAR retrieval algorithms commonly perform a combined estimation of fAPAR and Leaf Area Index (LAI). The standard MODIS Terra LAI/fAPAR product (MOD15A2, Collection 5) is used in this study; this product is available globally as 8-day composites at 1-km spatial resolution on a Sinusoidal grid. Data are provided in spatial tiles of about $1,200 \times 1,200 \text{ km}^2$ [16].

The estimation procedure retrieves LAI and fAPAR from the remotely-observed and atmospherically corrected Bidirectional Reflectance Distribution Function (BRDF) recorded by MODIS in 7 spectral bands by solving an

inverse problem. A numerical inversion of the three-dimensional radiation transfer process through the canopy system is solved by splitting it into two separate sub-problems: i) the radiation field in the canopy calculated for a black surface, and ii) the radiation field in the same medium (with the black surface) generated by anisotropic sources located at the canopy bottom [17].

Once information on the canopy structure is available, the solution to these problems is obtainable. Hence, a Look-Up-Table (LUT) approach is adopted by subdividing the vegetated land into eight-biome classes: grasses and cereal crops, shrubs, broadleaf crops, savanna, deciduous broadleaf forests, evergreen broadleaf forests, deciduous needle forests, evergreen needle forests.

The MOD15A2 product is generated daily and successively aggregated to 8-day composites by using a maximum composite method; quality assessment (QA) flags are included in the 8-day composition, and a back-up algorithm is triggered for low quality pixels to estimate LAI and fAPAR from vegetation indices. Data from MODIS-Terra are available from April 2000 to nowadays.

For the period 2001-2015, we downloaded the MOD15A2 tiles covering Europe (from 17 to 21 horizontal and from 02 to 05 vertical). A series of post-processing procedures was applied to the 8-day fAPAR tiles in order to obtain dekadal maps (3 maps per month, corresponding to the days: 1-10, 11-20 and 21-end of the month) over the European domain. First of all, the tiles were mosaicked and reprojected in the common lat/lon regular grid at 0.01 degree resolution. Hence, low quality data were masked out according to the QA flag and fAPAR estimates for each dekadal were obtained by means of an exponential smoothing (with smoothing parameter equal to 0.5) of the raw data [18]. The exponential smoothing allows removing likely outlier (i.e., cloud contaminated values) without compromising a near-real time delivery of the newly upcoming data.

A long-term average fAPAR dataset is reconstructed by simply averaging the 15 values available for each dekadal, obtaining an estimate of the mean fAPAR dynamic for each cell in the domain.

B. Fitting procedure

Ecological studies have shown clear temporal patterns in fAPAR time series, in which periods of relatively constant low and high values are linked by transition (smooth increasing/decreasing) periods; these patterns can be relatively well represented by means of a sequence of logistic functions [19].

This approach was introduced by [13] for an automatic application on MODIS Enhanced Vegetation Index (EVI) images, with the aims of modelling a single growth/senescence cycle from remotely sensed data. These authors suggest subdividing the full period into segments of sustained increasing/decreasing values, each of which can be fitted by the function:

$$y(t) = \frac{c}{1 + \exp(a + bt)} + d \quad (1)$$

where t is time in dekadal, d is the minimum fAPAR value observed in the segment, $c+d$ is the maximum fAPAR value, a and b are the fitting parameters obtained from a least squares regression of the reduced variable $Y = \ln[c/(fAPAR-d)] - 1$ vs. t .

The key transition dates are identified from the fitted values $y(t)$ as the local extrema in the rate of change in curvature (derivative of the angle of the unit tangent of the curve along the unit length of the curve), K' :

$$K' = b^3 cz \left\{ \frac{3z(1-z)(1+z)^3 [2(1+z)^3 + b^2 c^2 z]}{[(1+z)^4 + (bcz)^2]^{5/2}} - \frac{(1+z)^2 (1+2z-5z^2)}{[(1+z)^4 + (bcz)^2]^{3/2}} \right\} \quad (2)$$

where $z = \exp(a + bt)$. Equation (2) presents three extrema (see Figure 1), the first is the onset of increasing fAPAR (circle), the second is the inflection point (cross) and the third is the onset of the maximum fAPAR values (square). In case of a segment with decreasing fAPAR values, the first and the last extrema represent the end of the period with maximum values and the end of the decreasing, respectively.

The fitting procedure is preceded by a segmentation phase, in which the single decreasing/increasing periods are identified. In this preliminary step a 5-value moving window average is performed on the fAPAR data, and the independent segments are identified in correspondence of the changes from positive to negative slope [19].

III. RESULTS

As described in Section II.B, a preliminary analysis of the fAPAR dekadal average data was performed in order to detect the number of segments necessary for an accurate fitting of the fAPAR annual cycle. As depicted in Figure 2, this analysis shows how most of the domain is characterized by a single cycle with a distinct peak (2 segments), even if a significant fraction of the domain (around 15%) presents 2 different peaks (4 segments) within the annual cycle.

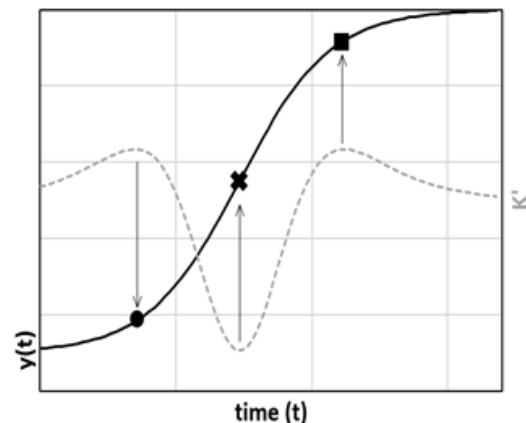


Figure 1. A schematic representation of the fitting procedure for a single segment (redrawn from [13]).

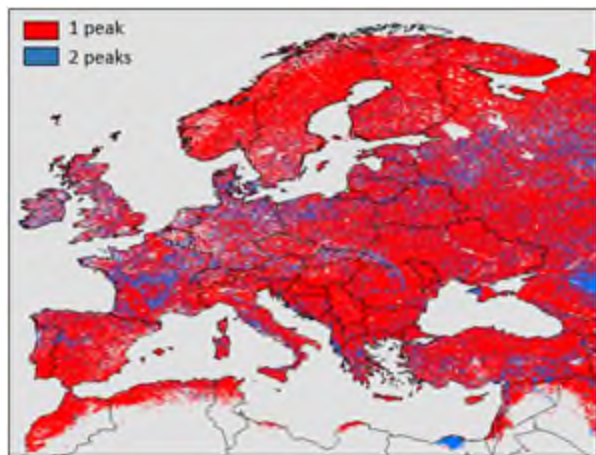


Figure 2. Spatial distribution of the cells with a single peak (in red) or with two peaks (in blue).

Distinct areas with two peaks in the processed window are the Nile (even if outside Europe) and Volga deltas, as well as some mountainous forests (i.e., Carpathian, Central Chain in Spain). It is worth to point out that a small fraction of the domain (around 8%) has no clear cycle according to our detection method, and an even smaller fraction ($< 2\%$) has more than 2 peaks (likely due to noisy time series); both areas were removed from the successive analyses.

The average fAPAR data were fitted according to a series of piecewise logistic functions, which number has been identified in the previous phase. For each cell, the key transition dates were evaluated, and two maps have been created as reported in Figure 3: a) starting Day Of the Year (DOY) of the increasing phase, and b) ending DOY of the decreasing phase.

The maps in Figure 3 show a quite large range of variability for both start and end dates, with distinct spatial patterns; in details, start date (Figure 3a) is early in the year (DOY 90) for Central Europe, is in the middle of the year for North Europe and quite late (DOY > 280) for the Mediterranean areas. Similarly, end date map (Figure 3b) shows a distinct North/South gradient, with end date just before summer for the Mediterranean countries, close to the end of the year for central Europe and around DOY 280-300 for North Europe. The North/South gradient observed in both transition dates is in general agreement with the expected phenological cycles for such regions.

The frequency distribution of the data in Figure 3a shows that the mode of the distribution is around DOY 130 ± 60 , even if a secondary small peaks can be observed at DOY = 290 (Mediterranean area). In contrast, the frequency distribution of the data in Figure 3b shows two overlapping bells around DOY 280 ± 15 and 330 ± 30 , corresponding to North-Central and South-Central Europe (respectively), and a quite small third peak at DOY 210 (Mediterranean areas).

The resulting length of the period between the start of the increasing and the end of the decreasing fAPAR (not shown) has a single peak distribution centered on DOY = 230 ± 70 days. It is worth to point out that data over North Europe are

severely affected by missing values during winter time (due to persistent cloud coverage and low solar angle), which likely affect the estimates of start/end dates and underestimate the length of the period between these two dates.

The most notable difference in the observed dynamics is that, while Central and North Europe fAPAR are relatively in-phase with the incoming solar radiation (with maximum values occurring during summer), the data over Mediterranean countries are off-phase (maximum values in early spring); the latter are mainly due to the severe water stress that occurs over these areas during summer. Overall, the observed dynamics are in agreement with the ground observed datasets (i.e., from flux towers) reported in [20] [21].

Finally, the plots in Figure 4 report three examples of fAPAR time series, as well as the transition points as detected by the applied methodology. The three sites were selected with the aim of illustrating the performance of the methodology over different conditions. These plots clearly highlight the good capability of the proposed procedure to identify the presence of single or multiple cycles, as well as of the piecewise logistic approach to capture the true dynamic of fAPAR. In particular, the plot in Figure 4c highlights the capability of the method to detect also the secondary transition points that occur between the two primary cycles, which can be used to further discriminate among different fAPAR time series behaviors.

IV. SUMMARY AND CONCLUSIONS

This paper evidences the flexibility of an approach based on piecewise logistic functions to automatically capture the dynamic of fAPAR over a large area, such as the European continent. The methodology allows identifying the main transition dates between increasing and decreasing periods in a consistent framework by exploiting the information content of the fAPAR dataset itself. The fitting of a continuous function for the computation of the transition dates, rather than the use of a discrete numerical detection, allows for a more coherent spatial definition of these dates.

The obtained results highlight a large variety of the vegetation dynamic within the studies domain, suggesting that the fAPAR anomalies occurring in the same decade over different areas may represent different effects on ecosystems due to the different phenological stages (e.g., green-up, senescence, etc.) at which those anomalies manifest. Additionally, the likely interannual variability of the detected transition dates should be analyzed in the current framework of climate change.

Improvements of the proposed modelling framework can be derived from quantitative comparisons of the retrieved key dates against ground observations; overall, these results can be considered a promising starting point for a more ecosystem-driven analysis of drought phenomena over Europe, which may be based on combining the information on the current phenological stage with the anomaly compared to the climatology.

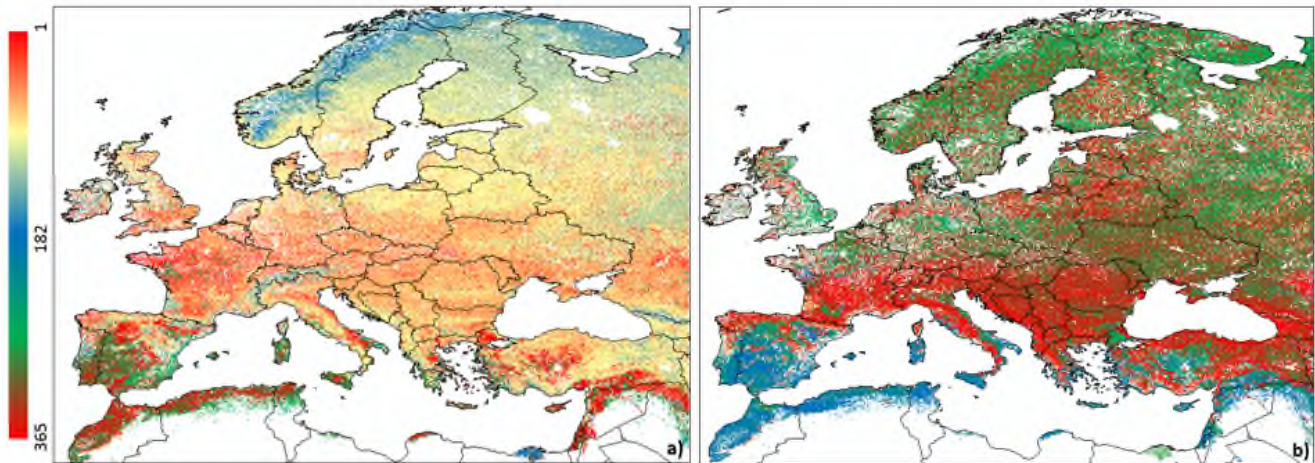


Figure 3. Spatial distribution of the two main transition dates (as Day Of the Year, DOY): (a) start of the fAPAR increasing period, (b) end of the fAPAR decreasing period.

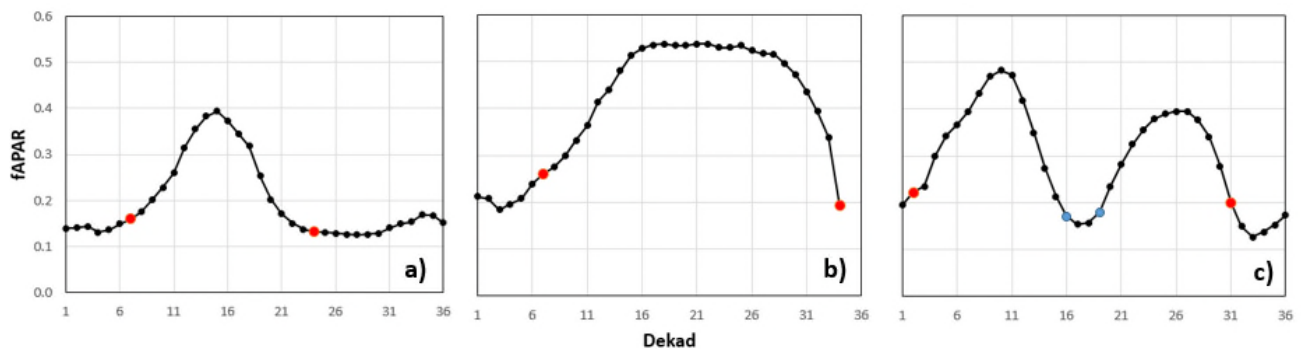


Figure 4. Example of fAPAR time series with main transition dates (red dots), as well as secondary ones (blue dots) in case of multiple peaks, for the sites: (a) South of Skopje (Macedonia), (b) North of Basel (Switzerland), and (c) Hatay region in Turkey.

ACKNOWLEDGMENT

The authors thank the NASA Land Process Distributed Active Archive Center (DAAC, <https://lpdaac.usgs.gov/>) for making the Terra MODIS satellite images freely available for download.

REFERENCES

[1] GCOS, "Summary report of the ninth session of the GCOS/GTOS terrestrial observation panel for climate," WMO/TD No.1371, Ispra (Italy), 28-29 March, 2007.

[2] N. Gobron et al., "The state vegetation in Europe following the 2003 drought," *Int. J. Remote Sens. Lett.*, vol. 26, 2005, pp. 2013-2020.

[3] S. Rossi and S. Niemeyer, "Drought monitoring with estimates of the fraction of absorbed photosynthetically-active radiation (fAPAR) derived from MERIS," in: *Remote Sensing of Drought: Innovative Monitoring Approaches*, B.D. Wardlow, M.C. Anderson and J.P. Verdin Eds., Boca Raton, FL, CRC Press, 2012.

[4] <http://edo.jrc.ec.europa.eu>. (Accessed on: May 24, 2016).

[5] G. Sepulcre-Canto, S. Horion, A. Singleton, H. Carrao, and J. Vogt, "Development of a combined drought indicator to detect agricultural drought in Europe," *Nat. Hazards Earth Syst. Sci.*, vol. 12, 2012, pp. 3519-3531.

[6] S. Rossi et al., "Potential of MERIS fAPAR for drought detection," in *Proceedings of the 2nd MERIS/(A)ATSR User Workshop*, ESA SP-666, H. Lacoste and L. Ouwehand Eds., Frascati, Italy, ESA Communication production Office, 2008, 6 pp.

[7] P.D. Jamieson, R.J. Martin, G.S. Francis, and D.R. Wilson, "Drought effects on biomass production and radiation-use efficiency in barley," *Field Crop. Res.*, vol. 43, n. 2-3, 1995, pp. 77-86.

[8] M. Linderman, Y. Zeng, and P. Rowhani, "Climate and land-use effects on interannual fAPAR variability from MODIS 250 m data," *Photogram. Eng. Remote Sens.*, vol. 76, n. 7, 2010, pp. 807-816.

[9] D. Lloyd, "A phenological classification of terrestrial vegetation cover using shortwave vegetation index imagery," *Int. J. Remote Sens.*, vol. 11, 1990, pp. 2269-2279.

[10] B.C. Reed et al., "Measuring phenological variability from satellite imagery," *J. Veg. Sci.*, vol. 7, 1994, pp. 703-714.

[11] E. Ivits et al., "Combining satellite derived phenology with climate data for climate change impact assessment," *Glob. Plan. Change*, vol. 88-89, 2012, pp. 85-97.

[12] M. Menenti, S. Azzali, W. Verhoef, and R. van Swol, "Mapping agroecological zones and time-lag in vegetation growth by means of Fourier-analysis of time-series of NDVI images," *Adv. Space Res.*, vol. 13, n. 5, 1993, pp. 233-237.

- [13] X. Zhang, et al., "Monitoring vegetation phenology using MODIS," *Remote Sens. Environ.*, vol. 84, 2002, pp. 471-475.
- [14] G.D. Badhwar, "Automatic corn-soybean classification using Landsat MSS data: II. Early season crop proportion estimation," *Remote Sens. Environ.*, vol. 14, 1984, pp. 31-37.
- [15] C. Atzberger, A. Klish, M. Mattiuzzi, and F. Vuolo, "Phenological metrics derived over the European continent from NDVI3g data and MODIS time series," *Remote Sens.*, vol. 6, n. 1, 2013, pp. 257-284.
- [16] R.B. Myneni, Y. Knyazikhin, J. Glassy, P. Votava, and N. Shabanov, "FPAR, LAI (ESDT: MOD15A2) 8-day Composite NASA MODIS Land Algorithm. User's Guide," 2003, 17 pp.
- [17] Y. Knyazikhin, J.V. Martonchik, R.B. Myneni, D.J. Diner, and S.W. Running, "Synergistic algorithm for estimating vegetation canopy leaf area index and fraction of absorbed photosynthetically active radiation from MODIS and MISR data," *J. Geophys. Res.*, vol. 103, 1998, pp. 32257-32274.
- [18] R.G. Brown and R.F. Meyer, "The fundamental theory of exponential smoothing," *Operat. Res.*, vol. 9, 1961, pp. 673-685.
- [19] D. Villegas, N. Aparicio, R. Blanco, and C. RoYo, "Biomass accumulation and main stem elongation of durum wheat grown under Mediterranean conditions," *Ann. Bot.*, vol. 88, 2001, pp. 617-627.
- [20] J.M. Paruelo, et al., "Temporal and spatial patterns of ecosystem functioning in protected arid areas in southeastern Spain," *Appl. Veg. Sci.*, vol. 8, 2005, pp. 93-102.
- [21] P. D'Odorico, et al., "Intercomparison of fraction of absorbed photosynthetically active radiation products derived from satellite data over Europe," *Remote Sens. Environ.*, vol. 142, 2014, pp. 141-154.

Aerial Image Mosaics Construction Using Heterogeneous Computing for Agricultural Applications

Leandro R. Candido

Embrapa Instrumentação
São Carlos, São Paulo 13560-970
Brazil

Email: l.candido@hotmail.com

Maximilian Luppe

Electrical Department - EESC - USP
São Carlos, São Paulo 13566-590
Brazil

Email: maxluppe@sc.usp.br

Lúcio A. C. Jorge

Embrapa Instrumentação
São Carlos, São Paulo 13560-970
Brazil

Email: lucio.jorge@embrapa.br

Abstract—In agriculture, image mosaics of forest and crop areas help different applications in precision farming that need to answer quickly. This work aims to show a different idea about image mosaic construction using heterogeneous computing in order to decrease the computational cost and giving a faster answer to the farmer about his crop.

Keywords—single board computer (SBC); ifc6540; mosaic; embedded system; sift; heterogeneous computing;

I. INTRODUCTION

Tarallo et al. [1] describe that by using mosaics in agriculture is possible to perform direct field inspections either during the growing cycle or days after the harvest, providing an accurate diagnosis of the growing area. From there, it is possible to draw recommendation maps: decompression, fertility and input application at variable rate.

The main problem for any image mosaic construction is associated with the images features. Scale Invariant Features Transform (SIFT) algorithm [2][3] is used to extract features from an image that it will be matching with features extracted from another image. This process has a higher computational effort in image mosaic construction. Heterogeneous computing can contribute to the mosaic construction by reducing the computational effort.

Advanced Micro Devices [4] defines heterogeneous computing as a system that is composed by one or more kind of processor, including Graphics Processing Units (GPU) and Field Programmable Gate Array (FPGA), besides conventional Central Processing Unit (CPU) and Digital Signal Processors (DSP). According to Kauer et al. [5], heterogeneous architecture has gained much space in the high performance computing area. This is due to the popularization of increasingly efficient graphics processors, that are every day more present in Single Board Computer (SBC). An SBC [6] is a computer where all necessary electronics components for its operation are on the same board. It is very useful in robotics applications, control system, automation and others.

This paper aims to introduce a new idea about image mosaic construction using heterogeneous computing, where SIFT algorithm will be implemented in GPU in order to reduce the computational effort. The paper is organized as follows. In Section II, it is described the Inforce 6540 SBC architecture and the Scale-Invariant Feature Transform. In Section III, the

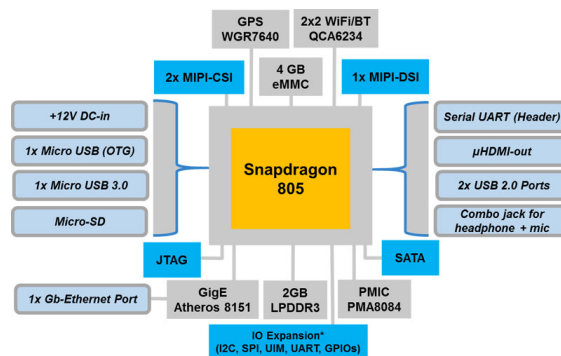


Figure 1. Inforce 6540 SBC Block Diagram

initial results are presented, and the conclusion and future works are described in Section IV.

II. MATERIAL AND METHODS

A. Inforce 6540 SBC (IFC6540)

IFC6540 is an SBC manufactured by Inforce Computing [7]. It is based on the first commercial processor with support for 4k Ultra HD technology, the Snapdragon 805 (APQ8084).

Figure 1 shows all the electronic components that IFC6540 provides for user.

Snapdragon 805 (APQ8084) is a processor developed by Qualcomm [8] in order to work with the technology 4K Ultra HD with capture, reproduction and video output 4K on mobile devices. This chip integrates connectivity and heterogeneous computing. In heterogeneous computing encapsulated in this chip, stands out:

- Quad core Krait 450 CPU 2.7GHz per core
- Adreno 420 GPU @4.8 Pixels/second
- Hexagon DSP v50 @600MHz

Figure 2 shows the Snapdragon 805 processor and its main components.

B. Scale-invariant feature transform (SIFT)

SIFT [2][3] is a method for extracting distinctive invariant features from images that can be used to perform reliable matching between different views of an object or scene. The

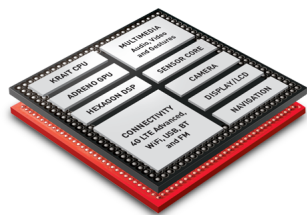


Figure 2. Snapdragon 805

features are invariant to image scale and rotation, and are shown to provide robust matching across a substantial range of affine distortion, change in 3D viewpoint, addition of noise, and change in illumination.

Lowe [2] describes four main steps used to generate the features in images. They are:

1) *Scale-space extrema detection*: This step aims to identify keypoints candidates that are invariant to scale and orientation. This is the most expensive process of all SIFT algorithm, because the original image is progressively blurred using Gaussian Blur and then the difference-of-Gaussian (DoG) function is applied.

2) *Keypoint localization*: By measuring the stability of keypoint, it is possible to determine the scale and location.

3) *Orientation assignment*: In this step, for each keypoint is assigned one or more orientation data based on local image gradient direction. This step aims to achieve invariance to rotation as the keypoint descriptor can be represented relative to this orientation.

4) *Keypoint descriptor*: Local gradients are measured around each keypoint to allow significant bright changes.

In this work, this method is used to attach different images where the keypoints are the same.

For this paper, there were two steps implemented based on Lowe's definition [2] as described early: step 1 (Scale-space extrema detection) and step 2 (Keypoint localization).

The partial implementation is shown in next section.

III. INITIAL RESULTS

C++ programming language together with an open source computer vision library called OpenCV [9] were used for SIFT algorithm implementation. This library provides some ready image functions like Gaussian filter (image convolution) and others functions.

Figure 3a shows an agriculture aerial image, registered using an Unmanned Aerial Vehicle (UAV), and Figure 3b shows the partial SIFT algorithm implemented where it is possible see the keypoint candidates after execution using processor Quad core Krait 450 CPU 2.7GHz of the SBC IFC6540.

IV. CONCLUSION AND FUTURE WORKS

This work is at the beginning. The first two SIFT steps, based on Lowes definition [2], were implemented and tested on a SBC IFC6540 board. The partial results are promising and it was possible to determine the scale and location of keypoints candidates, as shown in Figure 3b.

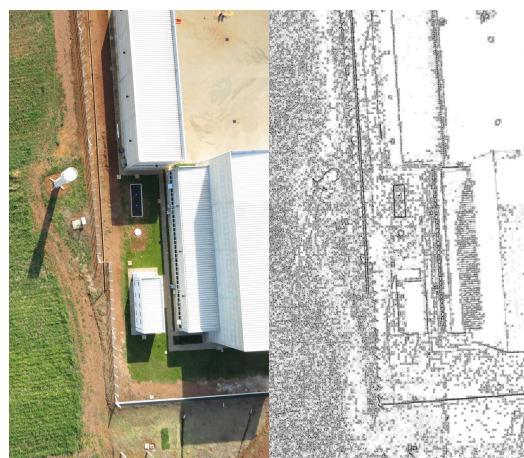


Figure 3. a) Original Image b) Keypoints Candidates.

All the steps will be implemented using the language OpenCL [10] to explore heterogeneous computing, transferring some functions to be processed on Adreno 420 GPU. The algorithm will also be optimized to improve performance, since the SIFT has higher computational cost in image mosaic construction, making it possible to obtain mosaic images on the fly.

ACKNOWLEDGMENT

The authors acknowledge the financial and institutional support given by the project CNPq 403426/2013-8 - Desenvolvimento de sistema de detecção, monitoração e controle de pragas e doenças nas lavouras - and Embrapa Instrumentação.

REFERENCES

- [1] Tarallo, A. S. and Paiva, M. S. V. and Jorge, L. A. C., "Mosaico automático de imagens agrícolas aéreas."
- [2] Lowe, D. G., "Distinctive image features from scale-invariant keypoints," International journal of computer vision, vol. 60, no. 2, 2004, pp. 91-110.
- [3] —, "Object recognition from local scale-invariant features," in Computer vision, 1999. The proceedings of the seventh IEEE international conference on, vol. 2. Ieee, 1999, pp. 1150-1157.
- [4] AMD. What is heterogeneous computing? Access date: 18 May. 2016. [Online]. Available: <http://developer.amd.com/resources/heterogeneous-computing/what-is-heterogeneous-computing/> (2015)
- [5] Kauer, A. U. and Siqueira, M. L., "Escalonamento em arquiteturas heterogêneas-apus," 13ª Escola de Alto Desempenho do Rio Grande do Sul, 2013, pp. 135-138.
- [6] Atwell, C. The biggest-little revolution: 10 single board computers for under \$100. Access date: Jan. 12, 2016. [Online]. Available: http://www.eetimes.com/document.asp?doc_id=1319262 (2013)
- [7] Inforce Computing. Inforce 6540 single board computer (sbc). Access date: Jan. 4 2016. [Online]. Available: <http://www.inforcecomputing.com/products/single-board-computers/6540-single-board-computer-sbc> (2015)
- [8] Qualcomm. Snapdragon 805. Access date: Jan. 4. 2016. [Online]. Available: <https://www.qualcomm.com/products/snapdragon/processors/805> (1985)
- [9] Bradski, G. and Kaehler, A., Learning OpenCV: Computer vision with the OpenCV library. " O'Reilly Media, Inc.", 2008.
- [10] Munshi, A. and Gaster, B. and Mattson, T. G. and Ginsburg, D., OpenCL programming guide. Pearson Education, 2011.